growth/differentiation factors: increased midkine expression in Wilms' tumor and other human carcinomas. *Cancer Res* 1993; **53**: 1281–5.
7 Aridome K, Tsutsui J, Takao S *et al.* Increased midkine gene expression in human gastrointestinal cancers. *Jpn J Cancer Res* 1995; **86**: 655–61.
8 Mishima K, Asai A, Kadomatsu K *et al.* Increased expression of midkine during the progression of human astrocytomas. *Neurosci Lett* 1997; **233**: 29–32.
9 O'Brien T, Cranston D, Fuggle S *et al.* The angiogenic factor midkine is expressed in bladder cancer, and overexpression correlates with a poor outcome in patients with invasive cancers. *Cancer Res* 1996; **56**: 2515–18.
10 Garver RI Jr, Radford DM, Donis-Keller H *et al.* Midkine and pleiotrophin expression in normal and malignant breast tissue. *Cancer* 1994; **74**: 1584–90.
11 Ye C, Qi M, Fan QW *et al.* Expression of midkine in the early stage of carcinogenesis in human colorectal cancer. *Br J Cancer* 1999; **79**: 179–84.
12 Konishi N, Nakamura M, Nakaoka S *et al.* Immunohistochemical analysis of midkine expression in human prostate carcinoma. *Oncology* 1999; **57**: 253–7.
13 Takei Y, Kadomatsu K, Matsuo S *et al.* Antisense oligodeoxynucleotide targeted to Midkine, a heparin-binding growth factor, suppresses tumorigenicity of mouse rectal carcinoma cells. *Cancer Res* 2001; **61**: 8486–91.
14 Takei Y, Kadomatsu K, Itoh H *et al.* 5'-,3'-inverted thymidine-modified antisense oligodeoxynucleotide targeting midkine. Its design and application for cancer therapy. *J Biol Chem* 2002; **277**: 23 800–6.
15 Ikematsu S, Nakagawara A, Nakamura Y *et al.* Correlation of elevated level of blood midkine with poor prognostic factors of human neuroblastomas. *Br J Cancer* 2003; **88**: 1522–6.
16 Ikematsu S, Yano A, Aridome K *et al.* Serum midkine levels are increased in patients with various types of carcinomas. *Br J Cancer* 2000; **83**: 701–6.
17 Ohira M, Oba S, Nakamura Y *et al.* Expression profiling using a tumor-specific cDNA microarray predicts the prognosis of intermediate risk neuroblastomas. *Cancer Cell* 2005; **7**: 337–50.
18 Warnat P, Oberthuer A, Fischer M *et al.* Cross-study analysis of gene expression data for intermediate neuroblastoma identifies two biological subtypes. *BMC Cancer* 2007; **7**: 89–99.
19 Joshi VV, Cantor AB, Brodeur GM *et al.* Correlation between morphologic and other prognostic markers of neuroblastoma. A study of histologic grade, DNA index, N-myc gene copy number, and lactic dehydrogenase in patients in the Pediatric Oncology Group. *Cancer* 1993; **71**: 3173–81.
20 Hann HW, Levy HM, Evans AE. Serum ferritin as a guide to therapy in neuroblastoma. *Cancer Res* 1980; **40**: 1411–3.
21 Zeltzer PM, Marangos PJ, Parma AM *et al.* Raised neuron-specific enolase in serum of children with metastatic neuroblastoma. A report from the Children's Cancer Study Group. *Lancet* 1983; **2**: 361–3.
22 Valentino L, Moss T, Olson E *et al.* Shed tumor gangliosides and progression of human neuroblastoma. *Blood* 1990; **75**: 1564–7.
23 Okabe-Kado J, Kasukabe T, Honma Y *et al.* Clinical significance of serum NM23-H1 protein in neuroblastoma. *Cancer Sci* 2005; **96**: 653–60.



doi: 10.1111/j.1349-7006.2008.00957.x

Vol 455|16 October 2008|doi:10.1038/nature07399

nature

LETTERS

# Oncogenic mutations of ALK kinase in neuroblastoma

Yuyan Chen[1,2,3]*, Junko Takita[1,2,3]*, Young Lim Choi[4]*, Motohiro Kato[1,3], Miki Ohira[5], Masashi Sanada[2,3,6], Lili Wang[2,3,6], Manabu Soda[4], Akira Kikuchi[7], Takashi Igarashi[1], Akira Nakagawara[5], Yasuhide Hayashi[8], Hiroyuki Mano[4,6] & Seishi Ogawa[2,3,6]

**Neuroblastoma in advanced stages is one of the most intractable paediatric cancers, even with recent therapeutic advances[1]. Neuroblastoma harbours a variety of genetic changes, including a high frequency of *MYCN* amplification, loss of heterozygosity at 1p36 and 11q, and gain of genetic material from 17q, all of which have been implicated in the pathogenesis of neuroblastoma[2–5]. However, the scarcity of reliable molecular targets has hampered the development of effective therapeutic agents targeting neuroblastoma. Here we show that the anaplastic lymphoma kinase (ALK), originally identified as a fusion kinase in a subtype of non-Hodgkin's lymphoma (NPM–ALK)[6–8] and more recently in adenocarcinoma of lung (EML4–ALK)[9,10], is also a frequent target of genetic alteration in advanced neuroblastoma. According to our genome-wide scans of genetic lesions in 215 primary neuroblastoma samples using high-density single-nucleotide polymorphism genotyping microarrays[11–14], the *ALK* locus, centromeric to the *MYCN* locus, was identified as a recurrent target of copy number gain and gene amplification. Furthermore, DNA sequencing of *ALK* revealed eight novel missense mutations in 13 out of 215 (6.1%) fresh tumours and 8 out of 24 (33%) neuroblastoma-derived cell lines. All but one mutation in the primary samples (12 out of 13) were found in stages 3–4 of the disease and were harboured in the kinase domain. The mutated kinases were autophosphorylated and displayed increased kinase activity compared with the wild-type kinase. They were able to transform NIH3T3 fibroblasts as shown by their colony formation ability in soft agar and their capacity to form tumours in nude mice. Furthermore, we demonstrate that downregulation of *ALK* through RNA interference suppresses proliferation of neuroblastoma cells harbouring mutated *ALK*. We anticipate that our findings will provide new insights into the pathogenesis of advanced neuroblastoma and that *ALK*-specific kinase inhibitors might improve its clinical outcome.**

To identify oncogenic lesions in neuroblastoma, we performed a genome-wide analysis of primary tumour samples obtained from 215 neuroblastoma patients using high-density single-nucleotide polymorphism (SNP) arrays (Affymetrix GeneChip 250K *Nspl*) (Supplementary Table 1). Twenty-four neuroblastoma-derived cell lines were also analysed (Supplementary Table 2). Interrogating over 250,000 SNP sites, this platform permits the identification of copy number changes at an average resolution of less than 12 kilobases (kb)[13,14].

Analysis of this large number of samples, consisting of varying disease stages, permitted us to obtain a comprehensive registry of genomic lesions in neuroblastoma (Supplementary Figs 1 and 2). A gain of chromosomes, often triploid or hyperploid (defined by mean copy number of >2.5), was a predominant feature of neuroblastoma genomes in the lower stages. Ploidy generally correlated with the clinical stage, where non-hyperploid cases were significantly associated with stage 4 disease ($P = 4.13 \times 10^{-5}$, trend test) (Supplementary Fig. 3 and Supplementary Table 3). 17q gains, frequently in multiple copies (3≤ copy number <5), were a hallmark of the neuroblastoma genome[4] and were found in most neuroblastoma cases. Copy number gains tended to spare chromosomes 3, 4, 10, 14 and 19 (Supplementary Figs 2 and 3). Notably, these chromosomes often had copy number losses including 1p (22.8%), 3p (8.8%), 4p (5.1%), 6q (7.0%), 10q (9.8%), 11q (19.5%), 14q (3.7%), 19p (7.4%) and 19q (5.1%), implicating the pathogenic role of 'relative' gene dosages.

After excluding known copy number variations, we identified a total of 28 loci undergoing high-grade amplifications (copy number ≥5) (Supplementary Table 4). These lesions fell into relatively small genomic segments, having a mean size of 361 kb, which accelerated the identification of gene targets in these regions (Supplementary Table 4 and Supplementary Fig. 4). The candidate gene targets included *TERT* (5p15.33), *HDAC3* (5q31.3), *IGF2* (11p15.1), *MYEOV* (11q13.3), *FGF7* (15q21.1) and *CDH13* (16q23.3). However, many of them were not recurrent but found only in a single case. Although the recurrent lesions were mostly explained by the amplification of *MYCN* at 2p24, as found in 50 out of 215 (23%) of the primary cases, we identified another peak of recurrent amplification at 2p23 (Fig. 1a), which consisted of amplicons in five primary cases and in one neuroblastoma-derived cell line, NB-1 (Supplementary Fig. 5). This peak was located at the centromeric margin of the common copy number gains in chromosome 2p, which was created by copy number gains in 109 samples mostly from non-hyperploid stage 4 cases. The minimum overlapping amplification was defined by the amplicons found in the NB-1 cell line (Supplementary Fig. 5) and contained a single gene, the anaplastic lymphoma kinase (*ALK*), which has previously been reported to be overexpressed in neuroblastoma cases[15]. Although five of the six samples showing *ALK* amplification also had *MYCN* amplification, one primary case (NT056) lacked a *MYCN* peak and the amplification was confined to the *ALK*-containing locus. In interphase fluorescent *in situ* hybridization (FISH) analysis of NB-1, *MYCN* and *ALK* loci were amplified in separate amplicons (Fig. 1b), indicating that the 2p23 amplicons containing *ALK* were unlikely to represent merely 'passenger' events of *MYCN* amplification but actively contributed to the pathogenesis of neuroblastoma.

Because an oncogene can be activated by gene amplification and/or mutation, to search for possible mutations we performed DNA heteroduplex formation analysis[16] and genomic DNA sequencing for the exons 20 to 28 of *ALK*, which encompass the juxtamembrane and kinase domains (Supplementary Table 5). In total, we identified eight nucleotide changes in 21 neuroblastoma samples, 13 out of 215

[1]Department of Pediatrics, [2]Cell Therapy and Transplantation Medicine, [3]Cancer Genomics Project, Graduate School of Medicine, The University of Tokyo, Tokyo 113-8655, Japan. [4]Division of Functional Genomics, Jichi Medical University, Toguchi 329-0498, Japan. [5]Division of Biochemistry, Chiba Cancer Center Research Institute, Chiba 260-8717, Japan. [6]Core Research for Evolutional Science and Technology, Japan Science and Technology Agency, Saitama, 332-0012, Japan. [7]Division of Hematology/Oncology, Saitama Children's Medical Center, Saitama 339-8551, Japan. [8]Gunma Children's Medical Center, Shibukawa 377-8577, Japan.
*These authors contributed equally to this work.

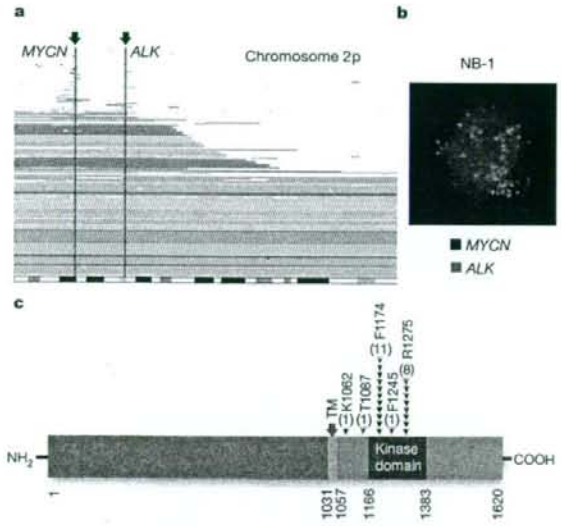


**Figure 1 | Common 2p gains/amplifications and *ALK* mutations in neuroblastoma samples.** **a**, Recurrent copy number gains on the 2p arm. High-grade amplifications are shown by light-red horizontal lines, whereas simple gains are shown by dark-red lines. Two common peaks of copy number gains and amplifications in the *MYCN* and *ALK* loci are indicated by arrows. The cytobands in 2p are shown at the bottom. **b**, Interphase FISH analysis of NB-1 showing high-grade amplification of *MYCN* (red) and *ALK* loci (green). The amplified *MYCN* locus appears as a single large signal. **c**, Distribution of the eight *ALK* mutations found in 21 neuroblastoma samples. The positions of the mutated amino acids are indicated by black (primary samples) and red (cell lines) arrowheads. The number of mutations at each site is shown at the top of the arrowheads. TM, transmembrane.

(6.1%) primary samples and 8 out of 24 (33%) cell lines, which resulted in seven types of amino acid substitutions at five different positions (Table 1 and Supplementary Fig. 6). They were not found in either the genomic DNA collected from 50 healthy volunteers or in the SNP databases at the time of preparing this manuscript. In fact, somatic origins of missense changes were confirmed in 9 out of 13 primary cases, for which DNA was obtained from the peripheral blood or the tumour-free bone marrow specimens (Supplementary Fig. 6). On the other hand, T1087I (ACC>ATC), found in case NT126, had a germline origin and thus it could not be determined whether the T1087I change was a rare non-functional polymorphism or represented a pathogenic germline mutation. For other changes found in three primary cases (NT128, NT217 and NT218) and cell lines, normal DNA was not available but they were likely to represent oncogenic mutations because they were identical to common somatic changes (F1174L or R1275Q) or shown to have oncogenic potential in functional assays (K1062M).

Most mutations occurred within the kinase domain (20 out of 22 or 91%), which clearly showed two mutation hotspots at F1174 and R1275 (Fig. 1c). A neuroblastoma-derived cell line, SJNB-2, had a homozygous *ALK* mutation of R1275Q, which was probably due to uniparental disomy of chromosome 2 (Supplementary Fig. 7a). Another case (NT074) harboured two different mutations, F1174L and R1275Q, but it remains to be determined whether both are on the same allele. ALK mutations within the kinase domain occurred at amino acid positions that are highly conserved across species and during molecular evolution (Supplementary Figs 8 and 9). According to the conserved structure of other insulin receptor kinases we predicted that F1174 is located at the end of the Cα1 helix, whereas the other two are on the two β-sheets: before the catalytic loop (β6, F1245) and within the activation loop (β9, R1275) (Supplementary Fig. 7b, c)[17]. Thus, conformational changes due to amino acid substitutions at these positions might be responsible for the aberrant activity of the mutant kinases.

**Table 1 | *ALK* mutations/amplifications in neuroblastoma samples**

| Sample | Age (months) | Stage | *MYCN** | Clinical outcome | Mutations/ amplifications | Nucleotide substitution | Origin of mutations |
|---|---|---|---|---|---|---|---|
| NT126 | 99 | 4 | − | Dead | T1087I | ACC>ATC | Germ line |
| NT218 | 8 | 1 | − | Alive | F1174L | TTC>TTG | ND |
| NT074 | 34 | 3 | + | Dead | F1174L | TTC>TTA | Somatic |
| | | | | | R1275Q | CGA>CAA | |
| NT160 | 12 | 4 | + | Dead | F1174L | TTC>TTA | Somatic |
| NT217 | 24 | 4 | + | Dead | F1174L | TTC>TTA | ND |
| NT190 | 48 | 4 | + | Alive | F1174L | TTC>TTA | Somatic |
| NT060 | 163 | 3 | − | Alive | F1174C | TTC>TGC | Somatic |
| NT162 | 28 | 4 | + | Dead | F1174V | TTC>GTC | Somatic |
| NT195 | 24 | 4 | + | Alive | F1245L | TTC>TTG | Somatic |
| NT055 | 6 | 3 | − | Alive | R1275Q | CGA>CAA | Somatic |
| NT128 | 8 | 4 | − | Dead | R1275Q | CGA>CAA | ND |
| NT164 | 54 | 4 | + | Dead | R1275Q | CGA>CAA | Somatic |
| NT200 | 133 | 4 | − | Dead | R1275Q | CGA>CAA | Somatic |
| SCMC-N5† | - | - | + | - | K1062M | AAG>ATG | ND |
| SJNB-4† | - | - | + | - | F1174L | TTC>TTA | ND |
| LAN-1† | - | - | + | - | F1174L | TTC>TTA | ND |
| SCMC-N2† | - | - | + | - | F1174L | TTC>TTA | ND |
| SK-N-SH† | - | - | − | - | F1174L | TTC>TTA | ND |
| SJNB-2†‡ | - | - | + | - | R1275Q | CGA>CAA | ND |
| LAN-5† | - | - | + | - | R1275Q | CGA>CAA | ND |
| TGW† | - | - | + | - | R1275Q | CGA>CAA | ND |
| NT204 | 12 | 1 | + | Alive | Amplification | - | - |
| NT056 | 11 | 3 | − | Dead | Amplification | - | - |
| NT071 | 36 | 3 | + | Alive | Amplification | - | - |
| NT165 | 19 | 4 | + | Dead | Amplification | - | - |
| NT169 | 7 | 4 | + | Dead | Amplification | - | - |
| NB-1† | - | - | + | - | Amplification | - | - |

ND, not determined.
* Presence (+) or absence (−) of *MYCN* amplification in FISH analysis. All cases where there was an absence of *MYCN* amplification (−) were also checked for possible *MYCN* mutations by sequencing of all *MYCN* exons, but no *MYCN* mutations were identified.
† Cell lines.
‡ Homozygous mutation.

*ALK* mutation highly correlated with *MYCN* amplification ($P = 1.55 \times 10^{-4}$, Fisher's exact test; Supplementary Table 6) where 14 out of 21 mutations coexisted with *MYCN* amplification. Regardless of the status of *MYCN* amplification, 12 of the 13 mutations were found in patients with advanced stage neuroblastoma (Table 1). However, whereas *MYCN* amplification and stage 4 were significant risk factors for poor survival, the mutation/amplification status of *ALK* was not likely to have a major impact on survival (Supplementary Fig. 10 and Supplementary Table 7), although the statistical power of the current analysis was largely limited in order to detect a marginal hazard.

To evaluate the impact of ALK mutations on kinase activity, we generated Flag-tagged constructs of ALK and its mutants, F1174L and K1062M, which were stably expressed in NIH3T3 cells, and examined their phosphorylation status and *in vitro* kinase activity. The ALK mutants stably expressed in NIH3T3 cells were phosphorylated according to western blot analysis using an antibody specific for phosphorylated ALK (anti-pY1604) and a PY20 blot after anti-Flag immunoprecipitation of the mutant kinases (Fig. 2a), whereas the wild-type kinase was not phosphorylated. The immunoprecipitated ALK mutants also showed increased tyrosine kinase activity *in vitro* when compared with wild-type ALK. This was shown using both a universal substrate for tyrosine kinase (poly-GluTyr) and the synthetic YFF peptide[18], which was derived from a sequence of the activation loop of *ALK* (Fig. 2b, c). In accordance with these findings, downstream molecules of ALK signalling including AKT, STAT3 and ERK[15] were activated in cells expressing mutant ALK, as shown by their increased phosphorylation (Fig. 2d).

Next, we investigated the oncogenic potential of these mutants. NIH3T3 cells stably expressing mutant kinases showed increased colony formation in soft agar compared with the wild-type protein (Fig. 3a and Supplementary Fig. 11). The tumorigenicity of these ALK mutants was further assayed by injecting $1.0 \times 10^7$ NIH3T3 cells into nude mice. The NIH3T3 cells transfected with the ALK mutants showed focus-forming capacity and developed subcutaneous tumours (6 out of 6 inoculations) 21 days after inoculation, whereas the mock and wild-type ALK-transfected cells did not (0 out of 6 inoculations) (Fig. 3b, c). Finally, we examined the effect of ALK inhibition on the proliferation of neuroblastoma-derived cell lines. RNA interference (RNAi)-mediated *ALK* knockdown resulted in reduced cell proliferation of SK-N-SH cells harbouring the F1174L mutation, but the effects were less clear in wild-type ALK-expressing LAN-2 cells (Fig. 3d, e). Of particular interest is a recent report that 5 out of 17 neuroblastoma-derived cell lines, including SK-N-SH and NB-1, frequently showed high sensitivity to the specific ALK inhibitor TAE684 (ref. 19).

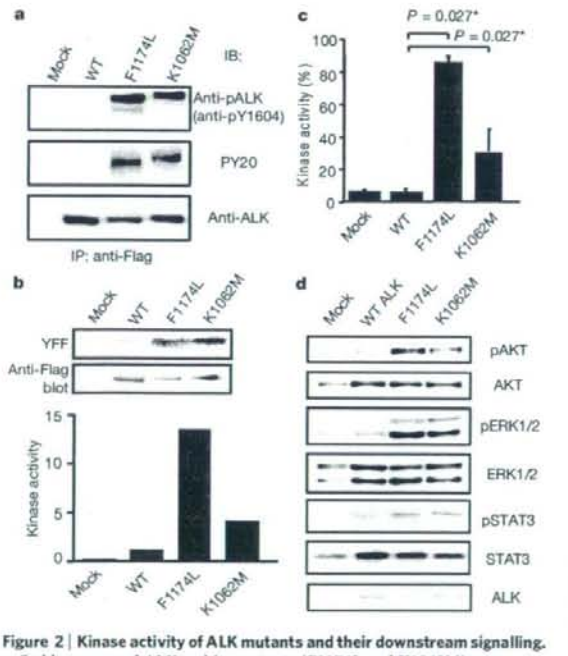


**Figure 2 | Kinase activity of ALK mutants and their downstream signalling.** **a**, Stably expressed ALK and its mutants (F1174L and K1062M) were immunoprecipitated with an anti-Flag antibody and subjected to western blot analysis with anti-pY1604 (upper panel) or PY20 (middle panel). An anti-ALK blot of precipitated kinases is also displayed (bottom panel). **b**, *In vitro* kinase assay for wild-type ALK kinase and its mutants using the synthetic YFF peptide as a substrate, where kinase activity is expressed as relative values to that for wild-type kinase based on the densities in the autoradiogram. **c**, Kinase activity was also assayed for the poly-GluTyr peptide. Significantly different measurements are indicated by asterisks with *P* values. Bars show mean (±s.d.) in three independent experiments. **d**, Western blot analyses of NIH3T3 cells expressing wild-type and mutant ALK for phosphorylated forms of AKT (pAKT), ERK (pERK1/2) and STAT3 (pSTAT3). The total amount of each molecule is also displayed (AKT, ERK1/2, and STAT3) together with an anti-ALK blot (ALK).

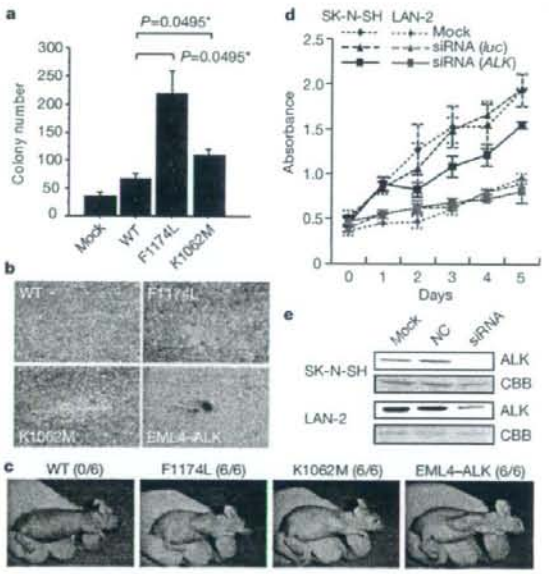


**Figure 3 | Oncogenic role of ALK mutations.** **a**, Colony assays for NIH3T3 cells stably expressing wild-type as well as mutant ALK (F1174L and K1062M). The average numbers of colonies in triplicate experiments are plotted and standard deviation is indicated. Results showing statistically significant differences as compared with experiments using wild-type ALK are indicated by asterisks with *P* values. **b**, **c**, NIH3T3 cells were transfected with wild-type and mutant ALK (F1174L, K1062M and EML4–ALK) and subjected to a focus forming assay (**b**) as well as an *in vivo* tumorigenicity assay in nude mice (**c**). **d**, Effect of RNAi-mediated ALK knockdown on cell proliferation in neuroblastoma cell lines expressing either the F1174L mutant (SK-N-SH) or wild-type ALK (LAN-2). Cell growth was measured using the Cell Counting Kit-8 after knockdown experiments using *ALK*-specific siRNAs (siRNA *ALK*), control siRNAs (siRNA *luc*), or mock experiments, where absorbance was measured in triplicate and averaged for each assay. To draw growth curves, the mean ± s.d. of the averaged absorbance in three independent knockdown experiments is plotted. **e**, Successful knockdown of ALK protein was confirmed by anti-ALK blots (ALK) using Coomassie brilliant blue G-250 (CBB) staining as loading controls. NC, control siRNA; siRNA, *ALK* siRNA.

Through the genome-wide analysis of genetic lesions in neuroblastoma, we identified novel oncogenic *ALK* mutations in advanced neuroblastoma. Combined with the cases having a high-grade amplification of the *ALK* gene, aberrant ALK signalling was likely to be involved in 11% (16 out of 151) of the advanced neuroblastoma cases. Because ALK kinase has been shown to be deregulated only in the form of a fusion kinase in human cancers, including lymphoma and lung cancer, the identification of oncogenic mutations in *ALK* not only increases our understanding of the molecular pathogenesis of advanced neuroblastoma, but also adds a new paradigm to the concept of 'ALK-positive human cancers' in that the mutated *ALK* kinases themselves might participate in human cancers. Our results again highlight the power of genome-wide studies to clarify the genetic lesions in human cancers[20–22]. Given that *ALK* mutations are preferentially involved in advanced neuroblastoma cases having a poor prognosis, our findings implicate that *ALK* inhibitors may improve the clinical outcome of children suffering from intractable neuroblastoma.

## METHODS SUMMARY

Genomic DNA from 215 patients with primary neuroblastoma and 24 neuroblastoma-derived cell lines was analysed on GeneChip SNP genotyping microarrays (Affymetrix GeneChip 250K *Nsp*I). After appropriate normalization of mean array intensities, signal ratios were calculated between tumours and anonymous normal references in an allele-specific manner, and allele-specific copy numbers were inferred from the observed signal ratios based on the hidden Markov model using CNAG/AsCNAR software[13,14]. *ALK* mutations were examined by DNA heteroduplex analysis and/or genomic DNA sequencing[16]. Full-length cDNAs for mutant *ALK* were isolated by high-fidelity PCR and inserted into pcDNA3 and pMXS. The expression plasmids were transfected into NIH3T3 cells using Effectene Transfection Reagent (Qiagen) or by calcium phosphate methods[9]. Western blot analysis of mutant ALK kinases, *in vitro* kinase assays, and tumour formation assays in nude mice were performed as previously described[9]. This study was approved by the ethics boards of the University of Tokyo and of the Chiba Cancer Center Research Institute.

**Full Methods** and any associated references are available in the online version of the paper at www.nature.com/nature.

**Received 3 June; accepted 28 August 2008.**

1. Maris, J. M., Hogarty, M. D., Bagatell, R. & Cohn, S. L. Neuroblastoma. *Lancet* 369, 2106–2120 (2007).
2. Maris, J. M. *et al.* Loss of heterozygosity at 1p36 independently predicts for disease progression but not decreased overall survival probability in neuroblastoma patients: a Children's Cancer Group study. *J. Clin. Oncol.* 18, 1888–1899 (2000).
3. Attiyeh, E. F. *et al.* Chromosome 1p and 11q deletions and outcome in neuroblastoma. *N. Engl. J. Med.* 353, 2243–2253 (2005).
4. Bown, N. *et al.* Gain of chromosome arm 17q and adverse outcome in patients with neuroblastoma. *N. Engl. J. Med.* 340, 1954–1961 (1999).
5. Brodeur, G. M., Seeger, R. C., Schwab, M., Varmus, H. E. & Bishop, J. M. Amplification of N-myc in untreated human neuroblastomas correlates with advanced disease stage. *Science* 224, 1121–1124 (1984).
6. Shiota, M. *et al.* Anaplastic large cell lymphomas expressing the novel chimeric protein p80NPM/ALK: a distinct clinicopathologic entity. *Blood* 86, 1954–1960 (1995).
7. Morris, S. W. *et al.* Fusion of a kinase gene, ALK, to a nucleolar protein gene, NPM, in non-Hodgkin's lymphoma. *Science* 263, 1281–1284 (1994).
8. Fujimoto, J. *et al.* Characterization of the transforming activity of p80, a hyperphosphorylated protein in a Ki-1 lymphoma cell line with chromosomal translocation t(2;5). *Proc. Natl Acad. Sci. USA* 93, 4181–4186 (1996).
9. Soda, M. *et al.* Identification of the transforming *EML4–ALK* fusion gene in non-small-cell lung cancer. *Nature* 448, 561–566 (2007).
10. Rikova, K. *et al.* Global survey of phosphotyrosine signaling identifies oncogenic kinases in lung cancer. *Cell* 131, 1190–1203 (2007).
11. Kennedy, G. C. *et al.* Large-scale genotyping of complex DNA. *Nature Biotechnol.* 21, 1233–1237 (2003).
12. Matsuzaki, H. *et al.* Genotyping over 100,000 SNPs on a pair of oligonucleotide arrays. *Nature Methods* 1, 109–111 (2004).
13. Nannya, Y. *et al.* A robust algorithm for copy number detection using high-density oligonucleotide single nucleotide polymorphism genotyping arrays. *Cancer Res.* 65, 6071–6079 (2005).
14. Yamamoto, G. *et al.* Highly sensitive method for genomewide detection of allelic composition in nonpaired, primary tumor specimens by use of affymetrix single-nucleotide-polymorphism genotyping microarrays. *Am. J. Hum. Genet.* 81, 114–126 (2007).
15. Osajima-Hakomori, Y. *et al.* Biological role of anaplastic lymphoma kinase in neuroblastoma. *Am. J. Pathol.* 167, 213–222 (2005).
16. Donohoe, E. Denaturing high-performance liquid chromatography using the WAVE DNA fragment analysis system. *Methods Mol. Med.* 108, 173–187 (2005).
17. Hu, J., Liu, J., Ghirlando, R., Saltiel, A. R. & Hubbard, S. R. Structural basis for recruitment of the adaptor protein APS to the activated insulin receptor. *Mol. Cell* 12, 1379–1389 (2003).
18. Donella-Deana, A. *et al.* Unique substrate specificity of anaplastic lymphoma kinase (ALK): development of phosphoacceptor peptides for the assay of ALK activity. *Biochemistry* 44, 8533–8542 (2005).
19. McDermott, U. *et al.* Genomic alterations of anaplastic lymphoma kinase may sensitize tumors to anaplastic lymphoma kinase inhibitors. *Cancer Res.* 68, 3389–3395 (2008).
20. Garraway, L. A. *et al.* Integrative genomic analyses identify MITF as a lineage survival oncogene amplified in malignant melanoma. *Nature* 436, 117–122 (2005).
21. Mullighan, C. G. *et al.* Genome-wide analysis of genetic alterations in acute lymphoblastic leukaemia. *Nature* 446, 758–764 (2007).
22. Kawamata, N. *et al.* Molecular allelokaryotyping of pediatric acute lymphoblastic leukemias by high-resolution single nucleotide polymorphism oligonucleotide genomic microarray. *Blood* 111, 776–784 (2008).

**Supplementary Information** is linked to the online version of the paper at www.nature.com/nature.

**Acknowledgements** We thank H. P. Koeffler for critically reading and editing the manuscript. We also thank M. Matsumura, Y. Ogino, S. Ichimura, S. Sohma, E. Matsui, Y. Yin, N. Hoshino and Y. Nakamura for their technical assistance. This work was supported by the Core Research for Evolutional Science and Technology, Japan Science and Technology Agency and by a Grant-in-Aid from the Ministry of Health, Labor and Welfare of Japan for the third-term Comprehensive 10-year Strategy for Cancer Control.

**Author Contributions** Y.C., Y.L.C. and J.T. contributed equally to this work. M.K. and M.Sa. performed microarray experiments and subsequent data analyses. Y.C. and J.T. performed mutation analysis of *ALK*. Y.C., Y.L.C., J.T., M.So., L.W. and H.M. conducted functional assays of mutant ALK. A.N., M.O., T.I., A.K. and Y.H. prepared tumour specimens and were involved in statistical analysis. A.N., Y.H., H.M., J.T. and S.O. designed the overall study, and S.O. and J.T. wrote the manuscript. All authors discussed the results and commented on the manuscript.

**Author Information** The nucleotide sequences of *ALK* mutations detected in this study have been deposited in GenBank under the accession numbers EU788003 (K1062M), EU788004 (T1087I), EU788005 (F1174L; TTC/TTA), EU788006 (F1174L; TTC/TTG), EU788007 (F1174C), EU788008 (F1174V), EU788009 (F1245L) and EU788010 (R1275Q). The copy number data as well as the raw microarray data will be accessible from http://www.ncbi.nlm.nih.gov/geo/ with the accession number GSE12494. Reprints and permissions information is available at www.nature.com/reprints. Correspondence and requests for materials should be addressed to S.O. (sogawa-tky@umin.net) or Y.H. (hayashiy-tky@umin.ac.jp).

## METHODS

**Specimens.** Primary neuroblastoma specimens were obtained during surgery or biopsy from patients who were diagnosed with neuroblastoma and admitted to a number of hospitals in Japan. In total, 215 primary neuroblastoma specimens were subjected to SNP array analysis after informed consent was obtained from the parents of each patient. The patients were staged according to the International Neuroblastoma Staging System[23]. The clinicopathological findings are summarized in Supplementary Table 1. Twenty-four neuroblastoma-derived cell lines were also analysed by SNP array analysis (Supplementary Table 2). The SCMC-N2, SCMC-N4 and SCMC-N5 cell lines were established in our laboratory[24,25]. The SJNB series of cells and the UTP-N-1[26] cell line were gifts from A. T. Look and A. Inoue, respectively. The other cell lines used were obtained from the Japanese Cancer Resource Cell Bank (http://cellbank.nibio.go.jp/).

**Microarray analysis.** High molecular mass DNA was isolated from tumour specimens as well as from the peripheral blood or the bone marrow as described previously[24]. The DNA was subjected to SNP array analysis using Affymetrix GeneChip Mapping 50K and/or 250K arrays (Affymetrix) according to the manufacturer's suggested protocol. The scanned array images were processed with Gene Chip Operation software (GCOS)[13], followed by SNP calls using GTYE. Genome-wide copy number measurements and loss of heterozygosity detection were performed using CNAG/AsCNAR algorithms[14], which enabled an accurate determination of allele-specific copy numbers.

**Confirmation of SNP array data.** FISH and/or genomic PCR analysis confirmed the results of SNP array analyses as described previously[13]. PCR primer sets were designed to amplify several adjacent fragments inside and outside of the homozygously deleted regions in tumour samples.

**Mutation analysis.** Mutations in the *ALK* gene were examined in 239 neuroblastoma samples, including 24 cell lines, by denaturing high-performance liquid chromatography (DHPLC) using the WAVE system (Model 4500; Transgenomic) according to the manufacturer's suggested protocol[16]. The samples showing abnormal conformations were subjected to direct sequencing analysis using an ABI PRISM 3100 Genetic Analyser (Applied Biosystems). Using direct sequencing, mutation analysis of *MYCN* was also performed in seven cases with *ALK* alterations but not *MYCN* amplification. The primer sets used in this study are listed in Supplementary Table 5.

**Transforming potential of *ALK* mutants.** Total RNA was extracted from SJNB-1 (wild type), SCMC-N2 (F1174L) and SCMC-N5 (K1062M) cells as described previously[26]. First-strand cDNA was synthesized from RNA using Transcriptor Reverse Transcriptase and an oligo (dT) primer (Roche Applied Science). The resulting cDNA was then amplified by PCR using the KOD-Plus-Ver.2 DNA polymerase (Toyobo) and the primers sense 5′-TCAGAAGCTTTACCAAGGACTGTTCAGAGC-3′ and antisense 5′-AATTGCGGCCGCTACTTGTCATCGTCGTCCTTGTAGTCGGGCCCAGGCTG GTTCATGC-3′, thereby introducing a HindIII site at the 5′ terminus and a NotI site and a Flag sequence at the 3′ terminus. The HindIII–NotI fragments of *ALK* cDNA were subcloned into pcDNA3 to generate expression plasmids. After resequencing to confirm that they had no other mutations, the *ALK* plasmids were used for transfection into NIH3T3 cells using Effectene Transfection Reagent (Qiagen) according to the suggested manufacturer's protocol. The transfected NIH3T3 cells were selected in 800 μg $ml^{-1}$ G418 for 2 weeks to obtain stably expressing clones.

To evaluate the phosphorylation status of ALK mutants, the cell lysates of stable clones were immunoprecipitated with antibodies to Flag (Sigma) and the resulting precipitates were subjected to western blot analysis with the antibody specific to pTyr 1604 (Cell Signaling Technology) of ALK and the generic anti-phosphotyrosine antibody (PY20). The *in vitro* kinase activity of ALK mutants was measured using a non-radioactive isotope solid-phase enzyme-linked immunosorbent assay using the Universal Tyrosine Kinase Assay kit (Takara) according to the manufacturer's suggested protocol. We also performed the *in vitro* kinase assay with the synthetic YFF peptide (Operon Biotechnologies) as described previously[18]. For anchorage-independent growth analysis, $1 \times 10^3$ stably transfected NIH3T3 cells were mixed in 0.3% agarose with 10% FBS-DMEM and plated on 0.6% agarose-coated 35-mm dishes. After culture for 28 days, the colonies of >0.1 mm in diameter were counted. The quantification of the colonies was from three independent experiments. To investigate the downstream signalling of ALK, western blot analysis was performed using the anti-ERK1/2, anti-phospho-ERK1/2, anti-AKT, anti-phospho-AKT, anti-STAT3 and anti-phospho-STAT3 antibodies (Cell Signaling Technology)[15].

The cDNA mutant of *ALK* was also inserted into the pMXS plasmid and the constructs were introduced into NIH3T3 cells by the calcium phosphate method as described previously[9]. The cells were then either cultured for 21 days or injected subcutaneously at six sites in three nude mice.

**Inhibition of ALK through RNAi-mediated knockdown.** To suppress the expression of the ALK protein, two different pairs of *ALK* siRNAs (*ALK* siRNA1 and *ALK* siRNA2) were obtained (Qiagen)[15]. The sequences were 5′-GAGUCUGGCAGUUGACUUCdTdT-3′ for *ALK* siRNA1 and 5′-GCUCCGGCGUGCCAAGCAGdTdT-3′ for *ALK* siRNA2. A siRNA, targeting a sequence in firefly (*Photinus pyralis*) luciferase mRNA (*luc* siRNA), was used as a negative control (Qiagen)[15]. The sequences of *luc* siRNA were as follow: sense 5′-CGUACGCGGAAUACUUCGAdTdT-3′ and antisense 5′-UCGAAGUAUUCCGCGUACGdTdT-3′. Gene knockdown was achieved in SK-N-SH and LAN-2 cells using HiPerFect transfection reagent following the manufacturer's suggested instructions (Qiagen). To assess the effect of ALK knockdown on cell growth, these cells were seeded in 96-well plates at a concentration of $8.0 \times 10^3$ cells per well 24 h before transfection and assayed using the Cell Counting Kit-8 (Wako).

**Statistical analysis.** The significance of the correlation between *MYCN* amplification and *ALK* mutation was tested according to the conventional $2 \times 2$ contingency table using Fisher's exact test. The significance of the differences in kinase activity between wild-type and mutant ALK kinases was examined by the Mann–Whitney *U*-test based on the measured percentage activity of kinases in the precipitates of the corresponding samples. The significance of the differences in colony formation between wild-type and mutant ALK kinases was also examined by the Mann–Whitney *U*-test. The size of the hazards from possible risk factors, including International Neuroblastoma Staging System stages, *MYCN* status and *ALK* mutation/amplification were estimated by Cox regression analysis assuming a proportional hazard model using Stata software. Correlation between ploidy and clinical stage was tested by nptrend test.


23. Smith, E. I., Haase, G. M., Seeger, R. C. & Brodeur, G. M. A surgical perspective on the current staging in neuroblastoma—the International Neuroblastoma Staging System proposal. *J. Pediatr. Surg.* 24, 386–390 (1989).
24. Takita, J. *et al.* Allelotype of neuroblastoma. *Oncogene* 11, 1829–1834 (1995).
25. Takita, J. *et al.* Absent or reduced expression of the caspase 8 gene occurs frequently in neuroblastoma, but not commonly in Ewing sarcoma or rhabdomyosarcoma. *Med. Pediatr. Oncol.* 35, 541–543 (2000).
26. Takita, J. *et al.* Allelic imbalance on chromosome 2q and alterations of the caspase 8 gene in neuroblastoma. *Oncogene* 20, 4424–4432 (2001).

# ROS-Generating Mitochondrial DNA Mutations Can Regulate Tumor Cell Metastasis

Kaori Ishikawa,[1,2,3]* Keizo Takenaga,[4,5]* Miho Akimoto,[5] Nobuko Koshikawa,[4] Aya Yamaguchi,[1] Hirotake Imanishi,[1] Kazuto Nakada,[1,2] Yoshio Honma,[5] Jun-Ichi Hayashi[1]†

Mutations in mitochondrial DNA (mtDNA) occur at high frequency in human tumors, but whether these mutations alter tumor cell behavior has been unclear. We used cytoplasmic hybrid (cybrid) technology to replace the endogenous mtDNA in a mouse tumor cell line that was poorly metastatic with mtDNA from a cell line that was highly metastatic, and vice versa. Using assays of metastasis in mice, we found that the recipient tumor cells acquired the metastatic potential of the transferred mtDNA. The mtDNA conferring high metastatic potential contained G13997A and 13885insC mutations in the gene encoding NADH (reduced form of nicotinamide adenine dinucleotide) dehydrogenase subunit 6 (*ND6*). These mutations produced a deficiency in respiratory complex I activity and were associated with overproduction of reactive oxygen species (ROS). Pretreatment of the highly metastatic tumor cells with ROS scavengers suppressed their metastatic potential in mice. These results indicate that mtDNA mutations can contribute to tumor progression by enhancing the metastatic potential of tumor cells.

Because most chemical carcinogens bind preferentially to mitochondrial DNA (mtDNA) rather than to nuclear DNA (*1–3*), mtDNA is considered to be their major cellular target. It has been hypothesized that the resultant somatic mutations in mtDNA play a causal role in oncogenic transformation (*3*). Many subsequent studies have supported the idea of preferential accumulation of somatic mutations in tumor mtDNAs (*4–9*) and their contribution to tumor growth (*10, 11*). However, the apparent high frequency of mtDNA mutations in tumors could be due either to their stochastic accumulation (*12, 13*) or to laboratory errors (*14*). Moreover, if mtDNA mutations induce oncogenic transformation, all the offspring of a mother carrying such mutations should develop tumors due to the maternal inheritance of mtDNA (*15, 16*), but no bias toward maternal inheritance of tumor development has been reported. Nonetheless, it remains possible that mtDNA mutations are involved at a later stage of tumorigenesis, for example, in the development of metastatic potential. Recent studies demonstrated that dysfunction of the tricarboxylic acid cycle (TCA cycle) caused by mutations in nuclear DNA controls tumor phenotypes by the induction of a pseudo-hypoxic pathway under normoxic conditions (*17–19*). However, there has been no evidence of the involvement of mtDNA mutations in the development of metastatic potential or in the regulation of the pseudo-hypoxic pathway because of the difficulty of excluding possible involvement of nuclear DNA mutations in these processes (*20*).

We have examined the role of pathogenic mtDNA mutations in the development of tumor cell metastasis by studying two mouse tumor cell lines with different metastatic potentials (low metastatic P29 and high metastatic A11 cells) that originated from Lewis lung carcinoma (table S1) (*21–23*). We compared mitochondrial respiratory function by estimating the activities of respiratory complexes and found that P29 cells had normal activities, whereas A11 cells showed reduced activity of complex I (NADH dehydrogenase) (Fig. 1A). Complex I defects were also observed in high metastatic fibrosarcoma B82M cells but not in high metastatic colon adenocarcinoma LuM1 cells (Fig. 1A), which suggests that metastatic tumors are not always associated with complex I defects.

Because complex I consists of subunits encoded by both nuclear DNA and mtDNA (*24*), it was necessary to determine which genome, nuclear or mitochondrial, was responsible for the complex I defects and whether the complex I defects were responsible for the high metastatic potential. We addressed these issues by complete reciprocal exchange of mtDNAs between P29 and A11 cells by means of cell fusion to isolate transmitochondrial cybrids (fig. S1A and table S2) and examined whether complex I defects and metastatic potentials were cotransferred with the mtDNA. The results showed that complex I activity decreased in the cybrids with A11 mtDNA, whereas those with P29 mtDNA showed normal activity, irrespective of whether their nuclear DNAs were derived from P29 or A11 cells (Fig. 1B). Thus, complex I defects in the cybrids with A11 mtDNA appear to result from pathogenic mutations in their mtDNA, not in their nuclear DNA. We then examined the metastatic potential of the cybrids by inoculating them into a tail vein (to test "experimental" metastasis) and under the skin (to test "spontaneous" metastasis) of C57BL/6 mice and counting the number of nodules formed in the lung. Cybrids with A11 mtDNA acquired high metastatic potential, whereas cybrids with P29 mtDNA lost metastatic potential (table S2). These observations suggest that complex I defects and high metastatic potential are transferred simultaneously with the transfer of mtDNA from the A11 cells, whereas normal complex I activity and low metastatic potential are transferred simultaneously with the transfer of mtDNA from P29 cells. The mtDNA of A11 cells is therefore likely to harbor a mutation(s) responsible for complex I defects and metastasis.

We next examined whether these findings could be generalized to additional tumor cell lines. In these experiments, we transferred mtDNA from A11 cells into fibrosarcoma B82 cells with low metastatic potential and normal complex I activity, resulting in isolation of B82mtA11 cybrids (table S2). Conversely, we transferred mtDNA from B82M cells, which are derived from B82 cells but express high metastatic potential and complex I defects, into low metastatic P29 cells, resulting in isolation of P29mtB82M cybrids. Both B82mtA11 and P29mtB82M cybrids acquired complex I defects (Fig. 1C) and high metastatic potential (table S2), which suggests the cotransfer of these phenotypes and the mtDNAs from high to low metastatic cells of different tumor types. Notably, transfer of mtDNA from high metastatic A11 and B82M cells into nontransformed NIH3T3 cells did not induce tumorigenicity and metastatic potential in the resultant NIHmtA11 and NIHmtB82M cybrids (fig. S2A and table S2). Thus, pathogenic mtDNA mutations that induce complex I defects are present in A11 and B82M cells and control development of metastases; however, these mutations do not control the development of tumorigenicity and metastasis, at least in nontransformed NIH3T3 cells.

To identify the pathogenic mtDNA mutations that induced complex I defects and high metastatic potential in A11 and B82M cells, we compared the whole mtDNA sequences between P29 and A11 cells and between B82 and B82M cells. We conclude that a missense G13997A mutation in the A11 cells and a frame-shift 13885insC mutation in the B82M cells, both within the *ND6* (NADH dehydrogenase subunit 6) gene, are the pathogenic mutations that induce complex I defects, because these are the only mutations exclusively observed in the mtDNA of the high metastatic A11 cells and

[1]Graduate School of Life and Environmental Sciences, University of Tsukuba, 1-1-1 Tennodai, Tsukuba, Ibaraki 305-8572, Japan. [2]TARA Center, University of Tsukuba, 1-1-1 Tennodai, Tsukuba, Ibaraki 305-8572, Japan. [3]Japan Society for the Promotion of Science (JSPS), 8 Ichiban-cho, Chiyoda-ku, Tokyo 102-8472, Japan. [4]Division of Chemotherapy, Chiba Cancer Center Research Institute, 666-2 Nitona, Chuo-ku, Chiba 260-8717, Japan. [5]Shimane University Faculty of Medicine, 89-1 Enya-cho, Izumo, Shimane 693-8501, Japan.

*These authors contributed equally to this work.
†To whom correspondence should be addressed. E-mail: jih45@sakura.cc.tsukuba.ac.jp



MS no: RE1156906/CJH

B82M cells (Table 1). Restriction enzyme digestion of the polymerase chain reaction products amplified using mismatched primers suggests complete and reciprocal replacement of parental mtDNAs in our cybrids (fig. S3).

We next explored how the mutated mtDNA and resultant complex I defects regulate metastasis. Because complex I defects may lead to overproduction of reactive oxygen species (ROS) (*24*, *25*), we estimated the amounts of ROS (fig. S4), and found that the cybrids with the mutated mtDNA from A11 cells showed enhanced ROS production, whereas the cybrids without the mutated mtDNA from P29 cells did not (fig. S4B). Such cotransfer of ROS-producing properties to the cybrids along with the transfer of mtDNA with or without the mutation suggests that ROS overproduction is due to the G13997A mutation. ROS overproduction was also observed in the P29mtB82M and B82mtA11 cybrids (fig. S4C).

How does ROS overproduction regulate metastasis, and which nuclear genes (if any) are involved in this process? We have reported previously (*22*, *26*) that A11 cells, but not P29 cells, show resistance to hypoxia-induced apoptosis, accompanied by up-regulation of antiapoptotic MCL-1 (myeloid cell leukemia–1). Moreover, A11 cells showed higher expression levels of two genes associated with neoangiogenesis, HIF-1α (hypoxia-inducible factor–1α) and VEGF (vascular endothelial growth factor), in comparison with P29 cells (*27*). Thus, we focused here on the expression of these three nuclear-coded genes. We found that up-regulation of the MCL-1, HIF-1α, and VEGF was cotransferred when mutant mtDNA was transferred from A11 cells to the P29mtA11 and A11mtA11 cybrids. Down-regulation of three genes was cotransferred when wild-type mtDNA was transferred from P29 cells to the P29mtP29 and A11mtP29 cybrids (Fig. 2). Therefore, the mutated mtDNA and the resultant complex I defects induce up-regulation of the MCL-1, HIF-1α, and VEGF genes and are associated with high metastatic potential (fig. S1B). Gene expression profiling to compare P29mtP29 with P29mtA11 and A11mtP29 with A11mtA11 showed consistent up-regulation of other genes possibly related to metastasis in the cybrids with A11 mtDNA (table S3), which suggests involvement of additional genes in the mtDNA-mediated effects on metastasis.

To obtain direct evidence that ROS overproduction caused by the mutated mtDNA from A11 cells is responsible for high metastatic potential, we treated the P29mtA11 cybrids with ROS scavengers and examined their effects on the amounts of ROS and on the expression of the genes and the phenotypes related to metastasis. *N*-acetylcysteine (NAC), which has been used as an anticancer agent in preclinical models, was used as one ROS scavenger. The results showed

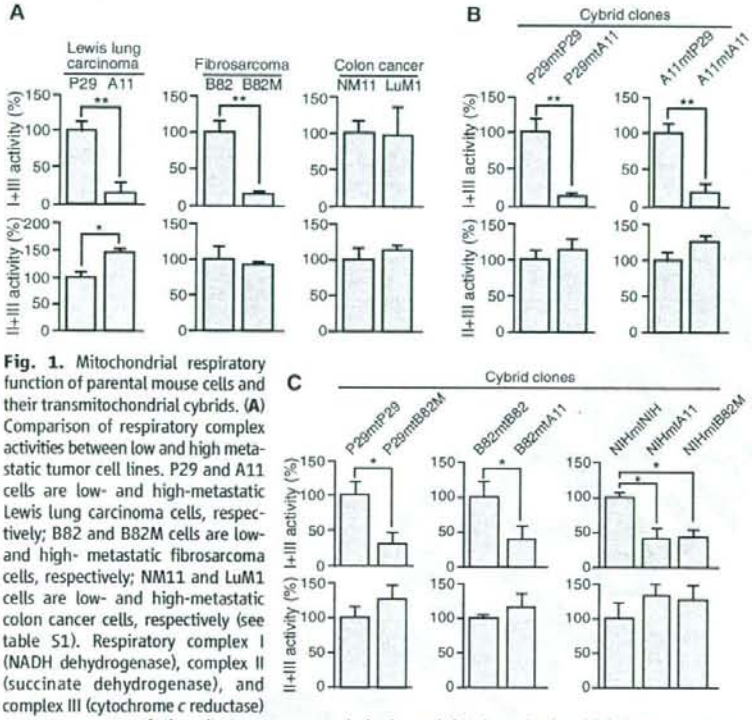


**Fig. 1.** Mitochondrial respiratory function of parental mouse cells and their transmitochondrial cybrids. **(A)** Comparison of respiratory complex activities between low and high metastatic tumor cell lines. P29 and A11 cells are low- and high-metastatic Lewis lung carcinoma cells, respectively; B82 and B82M cells are low- and high- metastatic fibrosarcoma cells, respectively; NM11 and LuM1 cells are low- and high-metastatic colon cancer cells, respectively (see table S1). Respiratory complex I (NADH dehydrogenase), complex II (succinate dehydrogenase), and complex III (cytochrome *c* reductase) are components of the electron-transport chain located in the mitochondrial inner membrane. Mitochondrial respiratory function was examined by estimating their activities. Because the activity of complexes II+III is normal in the A11 and B82M cells, the reduced activity of complexes I+III exclusively observed in the A11 and B82M cells should represent complex I defects. **(B)** Comparison of respiratory complex activities of the cybrids with mtDNA exchanged between low-metastatic P29 and high-metastatic A11 Lewis lung carcinoma cells. **(C)** Comparison of respiratory complex activities of the cybrids with mtDNA transferred from different types of tumor cells expressing high metastatic potential. Bars represent the mean ± SD ($n = 3$). *$P < 0.05$; **$P < 0.01$.

**Table 1.** Identification of pathogenic mutations by comparison of mtDNA sequences between low- and high-metastatic mouse tumor cells.

| Position | Gene | Amino acid change | Mouse strain | Cell lines | | | | | |
|---|---|---|---|---|---|---|---|---|---|
| | | | C57BL/6 | P29 | A11 | L929 | B82 | B82M | NIH/3T3 |
| T6589C | *COI* | V421A | T | T | T | C | C | C | T |
| G9348A | *COIII* | V248I | G | G | G | A | A | A | G |
| T9461C | *ND3* | Silent | T | C | C | C | C | C | C |
| 9821-PolyA | $tRNA^{Arg}$ | – | 8A | 9A | 9A | 10A | 10A | 10A | 10A |
| C11493A | *ND4* | P443T | C | A | A | C | C | C | C |
| A13672T | *ND6* | Silent | A | T | T | A | A | A | A |
| 13885insC | *ND6* | Frame-shift | – | – | – | – | – | C* | – |
| G13997A | *ND6* | P25L | G | G | A* | G | G | G | G |
| Accession No. | | | AY172335 | EU312160 | EU312161 | AJ489607 | EU315229 | EU315228 | AY999076 |

*The G13997A mutation in *ND6* is a missense mutation that changes the amino acid proline to leucine at a site that is highly conserved throughout vertebrates. The 13885insC mutation in *ND6* is a frame-shift mutation that has been previously reported as a pathogenic mutation that induces substantial complex I defects in some sublines of an L929 fibroblast cell line and A9 cells (*23*).



MS no: RE1156906/CJH

that treatment of the cybrids with NAC in cell culture reduced the amount of ROS (Fig. 3A) and down-regulated MCL-1 (Fig. 3B). Moreover, pretreatment of the cybrids with NAC reduced their metastatic potential in two mouse models (Fig. 3C). Similar results were obtained by treatment with another ROS scavenger, Ebselen, which is a mimic of glutathione peroxidase (Fig. 3). Thus, ROS overproduction caused by the mutated mtDNA induces a high metastatic potential, at least in part, by up-regulation of MCL-1. This idea is supported by the finding that down-regulation of MCL-1 in P29mtA11 cybrids by small interfering RNA also suppressed their metastatic potential (fig. S5). Moreover, NAC treatment suppressed the metastatic potential without reducing glycolytic activity (fig. S6), which suggests that metastasis is not caused by up-regulation of glycolysis.

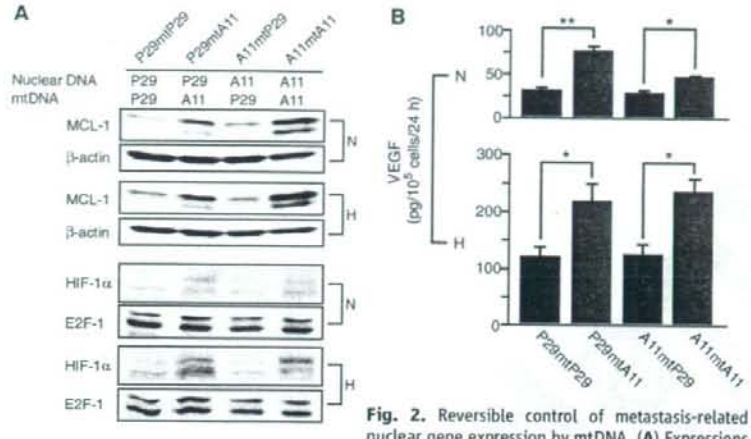


**Fig. 2.** Reversible control of metastasis-related nuclear gene expression by mtDNA. (**A**) Expressions of nuclear-coded MCL-1 and HIF-1α and (**B**) VEGF under normoxia (N) and hypoxia (H). As loading controls in the Western blots, we used β-actin for MCL-1 and E2F-1 for HIF-1α (A). In (B), blue bars represent cybrids carrying mtDNA from P29 cells (P29mtP29 and A11mtP29), and red bars represent cybrids carrying mtDNA from A11 cells (A11mtA11 and P29mtA11). Bars represent the mean ± SD ($n = 3$). $^*P < 0.01$; $^{**}P < 0.001$.

Contribution of mtDNA to tumor cell metastasis can be extended to human tumors, because the transfer of mtDNA from human breast cancer MDA-MB-231 cells expressing high metastatic potential into low metastatic HeLa cells induces complex I defects, increased ROS production, and high metastatic potential in HeLa cells (Fig. 4). These observations suggest that the mtDNA in MDA-MB-231 cells can promote metastasis, although we have not done the mtDNA sequencing. Therefore, the metastatic potential of all the mouse and human tumor cell lines that we examined was greatly enhanced by exchanging their endogenous mtDNA with mutant mtDNA that induces complex I–mediated ROS overproduction. Recent reports showed that a pathogenic mutation in the *ATP6* gene of human mtDNA generated ROS and enhanced tumor growth (*10*, *11*). However, in our experiments, the enhanced growth rate of primary tumors did not necessarily correlate with expression of the high metastatic potential in mouse tumors (fig. S2B).

This study partially resolves the debate on the relevance of mtDNA mutations in tumors (*4*–*14*) by showing that mutations in mtDNA can control the metastatic potential of certain tumor cells but that they do not confer tumorigenic potential to nontransformed mouse NIH3T3 cells. Moreover, reversible regulation of metastasis by the exchange of mtDNA between P29 and A11 cells and by treatment with ROS scavengers suggests that metastasis of these cells is regulated by ROS-mediated reversible up-regulation of nuclear genes but not by ROS-mediated acceleration of genetic instability. The mtDNA-mediated reversible con-

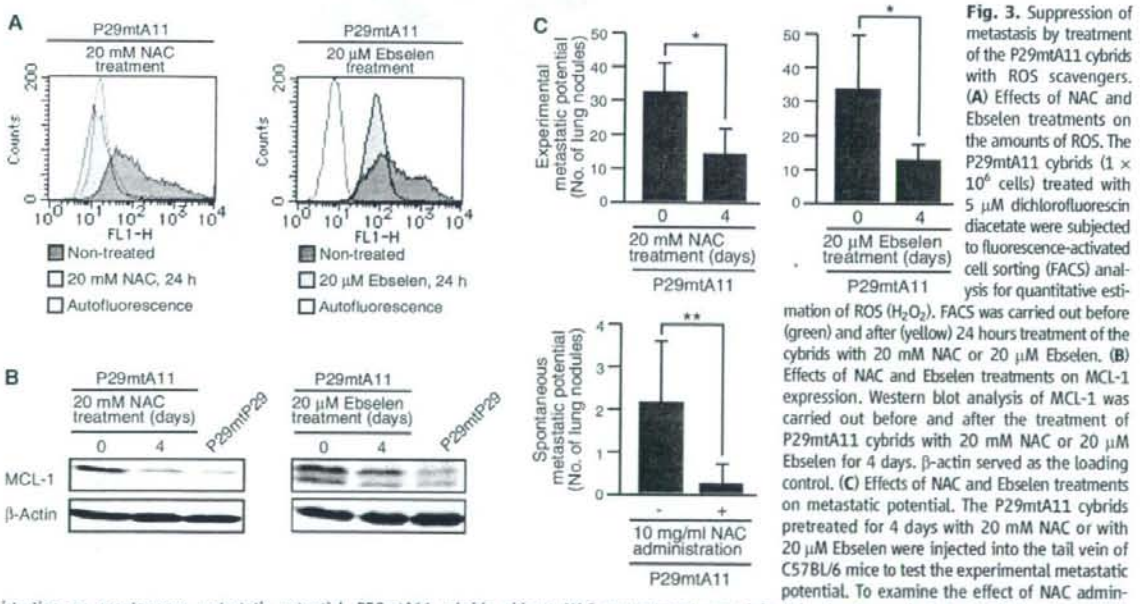


**Fig. 3.** Suppression of metastasis by treatment of the P29mtA11 cybrids with ROS scavengers. (**A**) Effects of NAC and Ebselen treatments on the amounts of ROS. The P29mtA11 cybrids ($1 \times 10^6$ cells) treated with 5 μM dichlorofluorescin diacetate were subjected to fluorescence-activated cell sorting (FACS) analysis for quantitative estimation of ROS ($H_2O_2$). FACS was carried out before (green) and after (yellow) 24 hours treatment of the cybrids with 20 mM NAC or 20 μM Ebselen. (**B**) Effects of NAC and Ebselen treatments on MCL-1 expression. Western blot analysis of MCL-1 was carried out before and after the treatment of P29mtA11 cybrids with 20 mM NAC or 20 μM Ebselen for 4 days. β-actin served as the loading control. (**C**) Effects of NAC and Ebselen treatments on metastatic potential. The P29mtA11 cybrids pretreated for 4 days with 20 mM NAC or with 20 μM Ebselen were injected into the tail vein of C57BL/6 mice to test the experimental metastatic potential. To examine the effect of NAC administration on spontaneous metastatic potential, P29mtA11 cybrids without NAC pretreatment were injected subcutaneously into C57BL/6 mice, which subsequently received 10 mg/ml NAC in drinking water ad libitum. Bars represent the mean ± SD ($n = 3$). $^*P < 0.05$; $^{**}P < 0.01$.



MS no: RE1156906/CJH

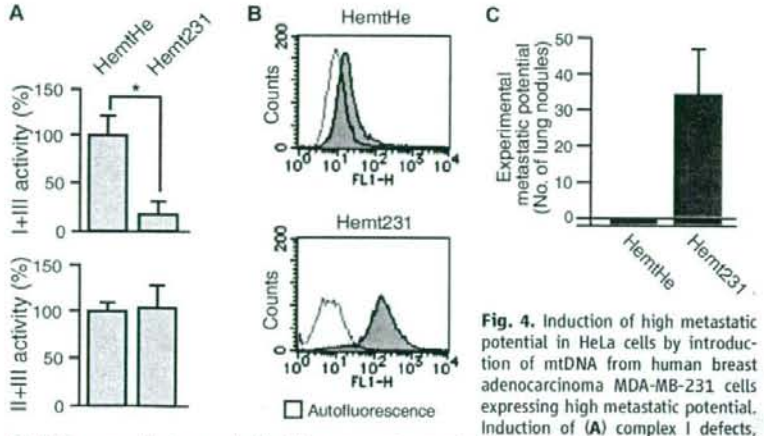


**Fig. 4.** Induction of high metastatic potential in HeLa cells by introduction of mtDNA from human breast adenocarcinoma MDA-MB-231 cells expressing high metastatic potential. Induction of **(A)** complex I defects, **(B)** ROS overproduction, and **(C)** high metastatic potential in the Hemt231 cybrids. HemtHe, HemtHe cybrids carrying nuclear DNA from $\rho^0$ HeLa cells and mtDNA from wild-type HeLa cells; Hemt231, Hemt231 cybrids carrying nuclear DNA from $\rho^0$ HeLa cells and mtDNA from MDA-MB-231 cells. Bars represent the mean ± SD ($n = 3$). *$P < 0.05$.

trol of metastasis, therefore, reveals a novel function of mtDNA and suggests that in such cases ROS scavengers may be therapeutically effective in suppressing metastasis.

### References and Notes


1. J. A. Allen, M. M. Coombs, *Nature* **287**, 244 (1980).
2. J. M. Backer, I. B. Weinstein, *Science* **209**, 297 (1980).
3. J. W. Shay, H. Werbin, *Mutat. Res.* **186**, 149 (1987).
4. K. Polyak *et al.*, *Nat. Genet.* **20**, 291 (1998).
5. M. S. Fliss *et al.*, *Science* **287**, 2017 (2000).
6. J. S. Penta, F. M. Johnson, J. T. Wachsman, W. C. Copeland, *Mutat. Res.* **488**, 119 (2001).
7. R. W. Taylor, D. M. Turnbull, *Nat. Rev. Genet.* **6**, 389 (2005).
8. A. M. Czarnecka, P. Golik, E. Bartnik, *J. Appl. Genet.* **47**, 67 (2006).
9. M. E. Gallardo *et al.*, *Hum. Mutat.* **27**, 575 (2006).
10. Y. Shidara *et al.*, *Cancer Res.* **65**, 1655 (2005).
11. J. A. Petros *et al.*, *Proc. Natl. Acad. Sci. U.S.A.* **102**, 719 (2005).
12. H. A. Coller *et al.*, *Nat. Genet.* **28**, 147 (2001).
13. R. W. Taylor *et al.*, *J. Clin. Invest.* **112**, 1351 (2003).
14. A. Salas *et al.*, *PLoS Med.* **2**, e296 (2005).
15. H. Kaneda *et al.*, *Proc. Natl. Acad. Sci. U.S.A.* **92**, 4542 (1995).
16. H. Shitara, J.-I. Hayashi, S. Takahama, H. Kaneda, H. Yonekawa, *Genetics* **148**, 851 (1998).
17. B. E. Baysal *et al.*, *Science* **287**, 848 (2000).
18. S. Niemann, U. Muller, *Nat. Genet.* **26**, 268 (2000).
19. E. Gottlieb, I. P. Tomlinson, *Nat. Rev. Cancer* **5**, 857 (2005).
20. L. H. Augenlicht, B. Heerdt, *Nat. Genet.* **28**, 104 (2001).
21. K. Takenaga, Y. Nakamura, S. Sakiyama, *Oncogene* **14**, 331 (1997).
22. M. Takasu, Y. Tada, J. O. Wang, M. Tagawa, K. Takenaga, *Clin. Exp. Metastasis* **17**, 409 (1999).
23. Materials and methods are available as supporting material on *Science* Online.
24. D. C. Wallace, *Science* **283**, 1482 (1999).
25. S. De Flora *et al.*, *Int. J. Cancer* **67**, 842 (1996).
26. N. Koshikawa, C. Maejima, K. Miyazaki, A. Nakagawara, K. Takenaga, *Oncogene* **25**, 917 (2006).
27. N. Koshikawa, A. Iyozumi, M. Gassmann, K. Takenaga, *Oncogene* **22**, 6717 (2003).


28. This work was supported by Grants-in-Aid for Scientific Research (S) from the Japan Society for Promotion of Science (JSPS), by Grants-in-Aid for Creative Scientific Research from JSPS, and by Grants-in-Aid for Scientific Research on Priority Areas from The Ministry of Education, Culture, Sports, Science and Technology of Japan (MEXT) to J.-I.H. This work was also supported by grants for a Research Fellowship from JSPS for Young Scientists to K.I. and by Grants-in-Aid for Third Term Comprehensive Control Research for Cancer from the Ministry of Health, Labour, and Welfare and for Scientific Research from MEXT to K.T. All animal experiments were performed in compliance with the institutional guidelines (Chiba Cancer Center and University of Tsukuba) for the care and use of laboratory animals.


### Supporting Online Material

www.sciencemag.org/cgi/content/full/1156906/DC1
Materials and Methods
Figs. S1 to S6
Tables S1 to S3
References


25 February 2008; accepted 25 March 2008
Published online 3 April 2008;
10.1126/science.1156906
Include this information when citing this paper.

Mitochondrion 8 (2008) 339–344

Contents lists available at ScienceDirect

Mitochondrion

journal homepage: www.elsevier.com/locate/mito

MitoMatters

# Reversible regulation of metastasis by ROS-generating mtDNA mutations

Kaori Ishikawa [a,b], Nobuko Koshikawa [c], Keizo Takenaga [d], Kazuto Nakada [a], Jun-Ichi Hayashi [a,*]

[a] Graduate School of Life and Environmental Sciences, University of Tsukuba, 1-1-1 Tennodai, Tsukuba, Ibaraki 305-8572, Japan
[b] Japan Society for the Promotion of Science (JSPS), 8 Ichiban-cho, Chiyoda-ku, Tokyo 102-8472, Japan
[c] Division of Chemotherapy, Chiba Cancer Center Research Institute, 666-2 Nitona, Chuo-ku, Chiba 260-8717, Japan
[d] Shimane University Faculty of Medicine, 89-1 Enya-cho, Izumo, Shimane 693-8501, Japan

ARTICLE INFO

*Article history:*
Received 30 June 2008
Received in revised form 24 July 2008
Accepted 30 July 2008
Available online 8 August 2008

*Keywords:*
mtDNA mutation
ROS overproduction
Nuclear-gene regulation
Metastasis
mtDNA transfer technology

ABSTRACT

It has been controversial whether mtDNA mutations are responsible for oncogenic transformation (normal cells to develop tumors), and for malignant progression (tumor cells to develop metastases). To clarify this issue, we created trans-mitochondrial cybrids with mtDNA exchanged between mouse tumor cells that express different metastatic phenotypes. The G13997A mutation in the *ND6* gene of mtDNA from high metastatic tumor cells reversibly controlled development of metastases by overproduction of reactive oxygen species (ROS), but did not control development of tumors. The mtDNA-mediated reversible control of metastasis reveals a novel function of mtDNA, and suggests that ROS scavengers may be therapeutically effective in suppressing metastasis.



## 1. Are mtDNA mutations involved in oncogenic transformation of normal cells to develop tumors?

Mitochondria of tumor cells have been reported to differ functionally and morphologically from those of normal cells (Pedersen, 1978). Moreover, many chemical carcinogens have been shown to bind preferentially to mtDNA rather than to nuclear DNA (Allen and Coombs, 1980; Backer and Weinstein, 1980). Therefore, mtDNA was considered to be the major cellular target of chemical carcinogens, and resultant creation of mutations in mtDNA could be responsible for oncogenic transformation of normal cells to develop tumors (Shay and Werbin, 1987). Although there has been no direct evidence for creation of mtDNA mutations by carcinogens, and for their contribution to develop tumors in mammalian cells, recent studies showed high frequencies of homoplasmic mutations in mtDNA of tumors rather than in mtDNA of normal tissues of the same patients (Polyak et al., 1998; Fliss et al., 2000). Many subsequent studies supported preferential accumulation of mutated mtDNAs in tumor cells (Penta et al., 2001; Taylor and Turnbull, 2005; Czarnecka et al., 2006; Gallardo et al., 2006).

On the contrary, our previous studies did not support the idea that mtDNA mutations are involved in tumor development (Hayashi et al., 1992; Hayashi et al., 1986; Hayashi et al., 1989). For example, we showed nuclear but not mitochondrial genome involvement in 3-methylcholanthrene (MCA)-induced expression of tumorigenicity by isolation of trans-mitochondrial cybrids using mtDNA exchange technology between normal mouse fibroblasts and their MCA-induced tumor cells (Hayashi et al., 1989): cybrids with nuclear DNA from MCA-induced tumor cells and mtDNA from normal cells expressed tumorigenicity, while those with nuclear DNA from normal cells and mtDNA from MCA-induced tumor cells did not express tumorigenicity. Similar results were obtained when mtDNA of HeLa cells was replaced by mtDNA from normal human skin fibroblasts: HeLa cybrids with nuclear DNA from HeLa cells and mtDNA from normal skin fibroblasts expressed tumorigenicity (Hayashi et al., 1986; Hayashi et al., 1992). All these observations suggested nuclear but not mitochondrial control of tumor development.

Our observations may represent some specific cases, and in most cases, mtDNA mutations control tumor development. However, this idea can be excluded by the following two reasons. First is that there is no statistical evidence for association of respiration defects and tumor development in the patients with mitochondrial diseases expressing significant respiration defects in their tissues. Of course, it is possible that some polymorphic mtDNA mutations that do not induce significant respiration defects and mitochondrial diseases could be responsible for tumor development. In this case, all family members sharing the same mothers carrying such mtDNA mutations, irrespective of whether they are pathogenic or polymorphic, should develop tumors, since mtDNA inherit maternally (Kaneda et al., 1995; Shitara et al., 1998). However, there has been no statistical evidence for the presence of maternal inheritance of tumor development.

* Corresponding author. Fax: +81 29 853 6614.
*E-mail address:* jih45@sakura.cc.tsukuba.ac.jp (J.-I. Hayashi).

1567-7249/$ - see front matter © 2008 Elsevier B.V. and Mitochondria Research Society. All rights reserved.
doi:10.1016/j.mito.2008.07.006

## 2. Are mtDNA mutations involved in malignant progression of tumor cells to develop metastasis?

Nonetheless, it is still possible that mtDNA mutations are involved in other processes than oncogenic transformation of normal cells to develop tumors, such as in the malignant progression of tumor cells to develop metastatic potential. Recent studies demonstrated that dysfunction of the TCA cycle caused by mutations in nuclear DNA controls tumor phenotypes by the induction of a pseudo-hypoxic pathway under normoxic conditions (Baysal et al., 2000; Niemann and Muller, 2000; Gottlieb and Tomlinson, 2005). However, there has been no direct evidence of the involvement of mtDNA mutations in malignant progression or in the regulation of the pseudo-hypoxic pathway, because of the difficulty of excluding possible involvement of nuclear DNA mutations in these processes (Augenlicht and Heerdt, 2001).

We addressed this issue by means of mtDNA exchange technology to examine the involvement of pathogenic mtDNA mutations in malignant progression of tumor cells to develop metastatic potential (Ishikawa et al., 2008). We used two mouse tumor cell lines expressing different metastatic potentials (low metastatic P29 cells and high metastatic A11 cells). Both cells are originated from the same Lewis lung carcinoma line formed in C57BL/6 mice (Takenaga et al., 1997; Takasu et al., 1999). We compared respiratory function by estimating the activities of respiratory complexes. The results showed that P29 cells had normal respiratory function, whereas A11 cells showed significant reduction of complex I (NADH dehydrogenase) activity.

Since complex I consists of subunits encoded by both nuclear DNA and mtDNA (Wallace, 1999), it was necessary to determine which genome, nuclear or mitochondrial, was responsible for the complex I defects, and whether the complex I defects were responsible for the high metastatic potential in A11 cells. We addressed these issues by complete and reciprocal exchange of mtDNAs between P29 and A11 cells by means of cell fusion technology to isolate trans-mitochondrial cybrids (Fig. 1). For complete and reciprocal mtDNA exchange between the parental cells, we isolated mtDNA-less ($\rho^0$) P29 and $\rho^0$ A11 cells, and then, used as mtDNA recipients, and generated four kinds of cybrids. P29mtP29 and P29mtA11 are the cybrids with nuclear genome from P29 cells and mitochondrial genome from P29 and A11 cells, respectively; A11mtA11 and A11mtP29 are the cybrids with nuclear genome from A11 cells and mitochondrial genome from A11 and P29 cells, respectively (Fig. 1).

Using these four cybrids, we examined whether complex I defects and metastatic potentials were co-transferred along with the mtDNA transfer. The results showed that complex I activity decreased in the cybrids with A11 mtDNA, whereas those with P29 mtDNA showed normal activity, irrespective of whether their nuclear DNAs were derived from P29 or A11 cells (Ishikawa et al., 2008). Thus, complex I defects in the cybrids with A11 mtDNA appear to result from pathogenic mutations in their mtDNA, not in their nuclear DNA. Then, we examined the metastatic potential of the cybrids by inoculating them into a tail vein (to test "experimental" metastasis) and under the skin (to test "spontaneous" metastasis) of C57BL/6 mice, and counting the number of nodules formed in the lung. Cybrids with A11 mtDNA (P29mtA11 and A11mtP29 cybrids) acquired high metastatic potential, whereas

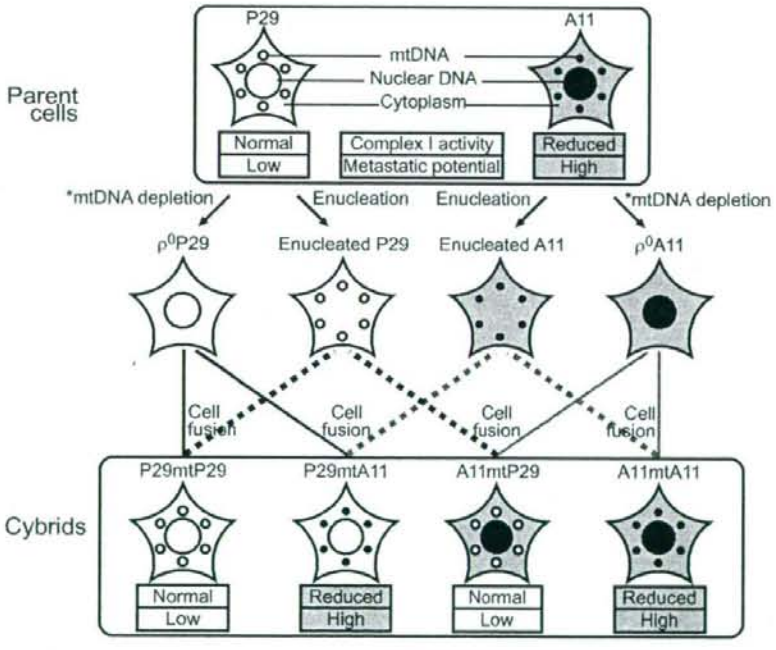


**Fig. 1.** Scheme for the isolation of trans-mitochondrial cybrids with completely exchanged mtDNA. *, Parental P29 and A11 cells were treated with ditercalinium to isolate $\rho^0$P29 and $\rho^0$A11 cells, which have no mtDNA, and then the G418-resistance plasmid was introduced into the $\rho^0$P29 and $\rho^0$A11 cells to permit isolation of $\rho^0$ cells resistant to G418. High metastatic potential and complex I defects are transferred with the transfer of mtDNA from the A11 cells, and low metastatic potential and normal complex I activity are transferred with the transfer of mtDNA from the P29 cells.

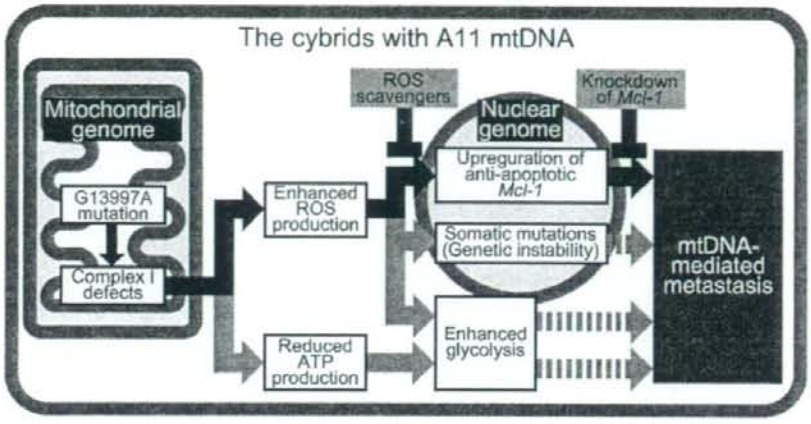


**Fig. 2.** Reversible control of metastasis by ROS-generating mtDNA mutations. Complex I defects caused by the G13997A mutation of mtDNA reversibly control metastasis by ROS overproduction and resultant upregulation of nuclear-coded genes related to metastasis, such as *Mcl-1*. The possibility that ROS overproduction controls metastasis by induction of genetic instability can be excluded from the evidence of reversible control of metastasis. Another possibility that ROS overproduction controls metastasis by induction of enhanced glycolysis also can be excluded from the evidence that ROS scavengers suppress metastasis without suppression of the enhanced glycolysis. Since complex I defects simultaneously induce enhanced glycolysis in addition to ROS overproduction, it is still possible that enhanced glycolysis caused by complex I defects alone is responsible for metastasis. This possibility can be excluded from the observation that metastasis is not induced in the P29mtΔ cybrids expressing enhanced glycolysis but not expressing ROS overproduction caused by the mtDNA with deletion mutation.

cybrids with P29 mtDNA (P29mtP29 and A11mtA11 cybrids) lost metastatic potential (Fig. 1).

### 3. Determination of the mtDNA mutations causing complex I defects and metastasis

These observations suggest that complex I defects and high metastatic potential are transferred simultaneously with the transfer of mtDNA from the A11 cells, whereas normal complex I activity and low metastatic potential are transferred simultaneously with the transfer of mtDNA from P29 cells. Thus, some pathogenic mtDNA mutations that induce complex I defects are present in A11 cells and control development of metastases.

Of course, it is possible that cytoplasmic factors transcribed from nuclear DNA of A11 cells, but not mtDNA of A11 cells control metastasis in P29mtA11 cybrids, since both nuclear-coded cytoplasmic factors and mtDNA were present in cytoplasts of A11 cells, and simultaneously introduced into the cybrids (see Fig. 1). However, this possibility can be excluded by the observations that A11mtP29 cybrids possessing nuclear-coded cytoplasmic factors of A11 cells do not express high metastatic potentials (Fig. 1). Thus, some mutated mtDNAs should be present in A11 cells and control complex I defects and metastasis.

To identify the presumptive pathogenic mutations in mtDNA from A11 cells, whole mtDNA sequences were compared between P29 and A11 cells. We found that the G13997A mutation in the A11 cells in the *ND6* (NADH dehydrogenase subunit 6) gene corresponded to pathogenic mutations that induced complex I defects by the following three reasons: (1) the G13997A mutation is the only mutations exclusively observed in the mtDNA of the high metastatic A11 cells; (2) The mutation occurred in the *ND6* gene, which encodes one of the subunits of complex I; (3) The mutation is a missense mutation that changes the amino acid proline to leucine, and is created at a site that is highly conserved throughout vertebrates (Ishikawa et al., 2008).

The G13997A mutation in A11 mtDNA can be effectively used to confirm complete and reciprocal replacement of parental mtDNAs in our cybrids. Since the mutation in A11 mtDNA creates an *Afl* II site in PCR products on amplification using mismatch primers, we carried out *Afl* II digestion of their PCR products. The results showed that the mtDNA in P29mtA11 and A11mtA11 cybrids possessed a homoplasmic G13997A mutation, and that mtDNA in the P29mtP29 and A11mtP29 cybrids did not (Ishikawa et al., 2008). These observations provide unambiguous evidence for complete and reciprocal replacement of parental mtDNAs between the P29 and A11 cells in the cybrids (Fig. 1).

### 4. How does the mutated mtDNA from A11 cells control metastasis?

The next question is how the mutated G13997A mtDNA and resultant complex I defects regulate metastasis (Fig. 2). Since complex I defects may lead to overproduction of ROS (Wallace, 1999), first we estimated the amounts of using a FACScan flow cytometer after incubation the cybrids with 2′,7′-dichlorofluorescein diacetate (DCFH-DA), and found that the cybrids with the mutated mtDNA from A11 cells showed enhanced ROS production, whereas the cybrids without the mutated mtDNA from P29 cells did not (Ishikawa et al., 2008). Such co-transfer of ROS-producing properties to the cybrids along with the transfer of mtDNA with or without the mutation suggests that ROS overproduction is due to the G13997A mutation (Ishikawa et al., 2008).

Then, we examined expression of anti-apoptotic MCL-1 and hypoxia-inducing factor HIF-1α, which are nuclear-coded genes related to metastasis, since previous reports showed that upregulation of MCL-1 and HIF-1α in highly metastatic A11 cells resulted in expression of resistance to hypoxia-induced apoptosis and enhanced neoangiogenesis, respectively, reading to expression of high metastatic potential in A11 cells (Takasu et al., 1999; Koshikawa et al., 2003, 2006). We focused here on the expression of these nuclear-coded genes that regulate hypoxia resistance and neoangiogenesis, and showed that upregulation of the MCL-1 and HIF-1α were observed in the cybrids with mtDNA from A11 cells, while their down regulation was observed in the cybrids with mtDNA from P29 cells (Ishikawa et al., 2008). Therefore, complex I defects induced by the mutated mtDNA and the resultant ROS overproduction may upregulate the nuclear-coded genes related to metastasis and lead to expression of high metastatic potential.

However, it is still possible that ROS overproduction regulates metastasis not by inducing upregulation of the nuclear-coded genes related metastasis, but by inducing genetic instability and extensive creation of somatic mutations in nuclear-coded genes related to metastasis (Fig. 2). Moreover, it is also possible that ROS overproduction regulates metastasis by induction of enhanced glycolysis (the Warburg effect). To address these important issues, we treated the P29mtA11 cybrids with ROS scavengers, and examined their effects on the amounts of ROS and on the expression of the genes and the phenotypes related to metastasis (Ishikawa et al., 2008). *N*-Acetylcysteine (NAC), which has been used as an anticancer agent, was used as one ROS scavenger. Treatment of the cybrids with NAC under the culture condition reduced the amount of ROS and downregulated MCL-1. Moreover, NAC treatment reduced both the experimental and spontaneous metastatic potentials. Similar results were obtained by treatment of the cybrids with another anti-oxidant, Ebselen (Ishikawa et al., 2008). Since the expression of the metastasis is reversibly controlled by ROS overproduction, ROS-induced genetic instability would not be responsible for metastasis. Moreover, we found that NAC treatment reduced both the amounts of ROS and metastatic potential without reducing glycolytic activity (Ishikawa et al., 2008). Thus, ROS overproduction induces high metastatic potential without stimulation of glycolysis (the Warburg effect) (Fig. 2).

Considering that complex I defects simultaneously induce respiration defects and enhanced glycolysis in addition to induce ROS overproduction, it would be necessary to examine whether enhanced glycolysis caused by complex I defects also could be responsible for metastasis (Fig. 2). For this, we isolated new cybrids named P29mtΔ with ΔmtDNA (mtDNA with a large-scale deletion mutation) by the fusion of $\rho^0$ P29 cells with platelets from mitomice carrying predominant amounts of ΔmtDNA. Accumulation of ΔmtDNA resulted in overall respiration defects by suppression of mitochondrial translation due the deletion of 5 mitochondrial tRNA genes in ΔmtDNA (Inoue et al., 2000; Nakada et al., 2001). As expected, the cybrids expressed overall respiration defects and enhanced glycolysis, but did not show ROS overproduction, probably due to overall respiration defects. Then, we examined their metastasis, and found that they did not show high metastatic potential (Ishikawa and Hayashi, unpublished observations). These observations suggest that the mutated A11 mtDNA control metastasis by ROS overproduction and resultant upregulation of nuclear-coded genes, such as MCL-1 (Fig. 2), but not by enhanced glycolysis.

The final possibility that we have to address is whether upregulation of nuclear-coded MCL-1 is responsible for expression of metastasis. Even though ROS overproduction induce upregulation of MCL-1 and metastasis, this does not necessarily mean that upregulation of MCL-1 is responsible for expression of metastasis. To test this possibility, we examined the effects of knock-down of MCL-1 by siRNA on metastasis. The results showed that downregulation of MCL-1 resulted in suppression of metastasis (Ishikawa et al., 2008). Thus, ROS overproduction caused by the mutated mtDNA induces a high metastatic potential, at least in part, by upregulation of MCL-1 (Fig. 2).

## 5. Generalization of the mtDNA-mediated metastasis

To generalize our concept to different tumor types, we used two pairs of mouse tumor cells, fibrosarcoma B82 and B82M cells, and colon cancer NM11 and LuM1 cells expressing low and high metastatic potentials, respectively. Complex I defects and ROS overproduction observed in high metastatic A11 cells were also observed in high metastatic fibrosarcoma B82M cells, but not in high metastatic colon cancer LuM1 cells, suggesting that high metastatic tumors are not always associated with complex I defects. Whole sequence analysis of mtDNA from B82M cells showed that 13885insC mutation in the *ND6* gene is responsible for complex I defects, ROS overproduction, and metastasis.

The question is whether high metastatic potential can be transferred to low metastatic tumor cells of different types along with the transfer of mtDNA from high metastatic tumor cells. First, we isolated $\rho^0$ B82 cells from low metastatic B82 cells as mtDNA recipients, and then, transferred A11 mtDNA into $\rho^0$ B82 cells, resulting in isolation of B82mtA11 cybrids. The cybrids possessed nuclear DNA from low metastatic B82 cells and mtDNA from high metastatic A11 cells. Conversely, we transferred mtDNA from B82M cells, which are derived from B82 cells but express high metastatic potential and complex I defects, into $\rho^0$ P29 cells, resulting in isolation of P29mtB82M cybrids. They possessed nuclear DNA from low metastatic P29 cells and mtDNA from high metastatic B82M cells. Both B82mtA11 and P29mtB82M cybrids acquired complex I defects and high metastatic potential, suggesting the co-transfer of these phenotypes and the mtDNAs from high to low metastatic cells of different tumor types (Ishikawa et al., 2008).

Contribution of mtDNA to metastasis of tumor cells can be extended to human cases: we used $\rho^0$ HeLa cells obtained from low metastatic HeLa cells as mtDNA recipients, and introduced the mtDNA from human breast cancer MDA-MB-231 cells expressing high metastatic potential. Resultant Hemt231 cybrids showed complex I defects, increased ROS production, and high metastatic potential. These observations suggest that the mtDNA in MDA-MB-231 cells can promote metastasis. Therefore, the metastatic potential of all mouse and human tumor cell lines we examined was greatly enhanced by exchanging their endogenous mtDNA with exogenous mtDNA carrying mutations that enhance ROS production by inducing significant complex I defects (Ishikawa et al., 2008).

## 6. Does the mutated mtDNA that induce metastasis in tumor cells also induce tumor development in normal cells?

Our previous report showed that the MCA-induced tumor cells retained normal respiratory function, and that mtDNA replacement of normal cells by the mtDNA from MCA-induced tumor cells did not induce tumor development (Akimoto et al., 2005). Considering that many cancer cells *in vivo* carry mtDNA mutations (Polyak et al., 1998; Fliss et al., 2000), they may become dependent on glycolytic pathway (the Warburg effect), and consume more glucose or other nutrients (Gottlieb and Tomlinson, 2005). To answer the question of whether defects in the mitochondrial respiratory function are related to tumor development, we should use tumor cells that have already acquired respiration defects and certain degree of activation of glycolytic pathway as mtDNA donors to examine its effect on oncogenic transformation of normal cells to tumor cells.

To address this issue, we used A11 cells as mtDNA donors to transfer mtDNA and examined whether the mutated mtDNA from high metastatic A11 cells can induce tumor development, when it was introduced into normal mouse cells. The G13997A mutation that induces respiration defects and metastasis in tumor cells may also induce tumor development in normal cells. We used NIH3T3 cells as normal cells, and isolated NIH3T3mtA11 cybrids by the fusion of $\rho^0$ NIH3T3 cells with enucleated A11 cells. The cybrids possessed nuclear DNA from NIH3T3 cells and mtDNA from A11 cells, and expressed complex I defects and ROS-overproduction, but did not express tumorigenicity and metastatic potential (Ishikawa et al., 2008). Thus, the mutated mtDNA in A11 cells controls metastatic potential, but does not control development of tumors at least in non-transformed NIH3T3 cells. These observations

again support our concept that mtDNA mutations are not involved in development of tumors (Akimoto et al., 2005).

## 7. Conclusion and future prospect

Our study can be summarized as follows:

(1) A missense G13997A mutation in the *ND6* gene of A11 mtDNA induces complex I defects, and reversibly controlled the metastatic potential, but does not control tumor development.
(2) Induction of metastasis is not due to enhanced glycolysis, but to ROS overproduction.
(3) ROS overproduction induces metastasis not by acceleration of genetic instability as usually proposed, but by reversible upregulation of nuclear-coded genes related to metastasis.
(4) ROS scavengers are therapeutically effective in suppressing mtDNA-mediated metastasis.

Thus, our study partly resolves the controversial issue on the relevance or irrelevance of mtDNA mutations in tumor development and/or tumor phenotypes by showing that mutations in mouse mtDNA control development of metastasis in tumor cells. In this case, the phenotype of tumor progression must inherit maternally. This issue could be resolved by the generation of trans-mitochondrial mice (mito-mice) by introducing the mutated G13997A mtDNA into mouse fertilized eggs or mouse female-type (XO-type) ES cells based on the procedures as reported previously (Inoue et al., 2000; Kasahara et al., 2006; Fan et al., 2008), to examine whether the mito-mice would develop tumors that are already metastatic. In humans, complex I defects caused by mtDNAs with pathogenic mutations and the resultant overproduction of ROS are reported to be associated with the pathogenesis in Leber's hereditary optic neuropathy (LHON; Wallace, 1999). Thus, statistical analysis would resolve the question of whether the patients with LHON develop cancers that are already metastatic.

Conventional mitochondrial theories propose that ROS-mediated genetic instability is responsible for aging, age-associated disorders, and tumor development (Wallace, 1999; Jacobs, 2003; Loeb et al., 2005). Although maternal inheritance is not reported in these phenotypes, this idea appears to be supported by a recent finding that mice expressing a proofreading-deficient version of mtDNA polymerase $\gamma$ show accelerated accumulation of somatic mutations in mtDNA, resulting in respiration defects and premature aging (Trifunovic et al., 2004). Subsequent studies have demonstrated the occurrence of premature aging in the absence of ROS overproduction (Kujoth et al., 2005; Trifunovic et al., 2005). Thus, it remains controversial whether ROS overproduction also induces premature aging phenotypes. This issue could be resolved by the generation of the mito-mice with the mutated G13997A mtDNA: these mice would continuously generate significant amounts of ROS in every tissue due to the mutated mtDNA, and would thus provide an ideal system to investigate precisely whether and how ROS overproduction results in the expression of LHON, the premature aging phenotypes, and the development of malignant tumors that are already metastatic.

## References


Akimoto, M., Niikura, M., Ichikawa, M., Yonekawa, H., Nakada, K., Honma, Y., Hayashi, J.-I., 2005. Nuclear DNA but not mtDNA controls tumor phenotypes in mouse cells. Biochem. Biophys. Res. Commun. 327, 1028–1035.

Allen, J.A., Coombs, M.M., 1980. Covalent binding of polycyclic aromatic compounds to mitochondrial and nuclear DNA. Nature 287, 244–245.

Augenlicht, L.H., Heerdt, B., 2001. Mitochondria: integrators in tumorigenesis? Nat. Genet. 28, 104–105.

Backer, J.M., Weinstein, I.B., 1980. Mitochondrial DNA is a major cellular target for a dihydrodiol-epoxide derivative of benzo(a)pyrene. Science 209, 297–299.

Baysal, B.E., Ferrel, I R.E., Willett-Brozick, J.E., Lawrence, E.C., Myssiorek, D., Bosch, A., van der Mey, A., Taschner, P.E., Rubinstein, W.S., Myers, E.N., 3rd Richard, C.W., Cornelisse, C.J., Devilee, P., Devlin, B., 2000. Mutations in SDHD, a mitochondrial complex II gene, in hereditary paraganglioma. Science 287, 848–851.

Czarnecka, A.M., Golik, P., Bartnik, E., 2006. Mitochondrial DNA mutations in human neoplasia. J. Appl. Genet. 47, 67–78.

Fan, W., Waymire, K.G., Narula, N., Li, P., Rocher, C., Coskun, P.E., Vannan, M.A., Narula, J., Macgregor, G.R., Wallace, D.C., 2008. A mouse model of mitochondrial disease reveals germline selection against severe mtDNA mutations. Science 319, 958–962.

Fliss, M.S., Usadel, H., Caballero, O.L., Wu, L., Buta, M.R., Eleff, S.M., Jen, J., Sidransky, D., 2000. Facile detection of mitochondrial DNA mutations in tumors and bodily fluids. Science 287, 2017–2019.

Gallardo, M.E., Moreno-Loshuertos, R., López, C., Casqueiro, M., Silva, J., Bonilla, F., Rodríguez de Córdoba, S., Enríquez, J.A., 2006. m.6267G>A: a recurrent mutation in the human mitochondrial DNA that reduces cytochrome c oxidase activity and is associated with tumors. Hum. Mutat. 27, 575–582.

Gottlieb, E., Tomlinson, I.P., 2005. Mitochondrial tumor suppressors: a genetic and biochemical update. Nat. Rev. Cancer 5, 857–866.

Hayashi, J.-I., Takemitsu, M., Nonaka, I., 1992. Recovery of the missing tumorigenicity in mitochondrial DNA-less HeLa cells by introduction of mitochondrial DNA from normal cells. Somat. Cell Mol. Genet. 18, 123–129.

Hayashi, J.-I., Werbin, H., Shay, J.W., 1986. Effects of normal human fibroblast mitochondrial DNA on segregation of HeLaTG mitochondrial DNA and on tumorigenicity of HeLaTG cells. Cancer Res. 46, 4001–4006.

Hayashi, J.-I., Yonekawa, H., Tagashira, Y., 1989. Nuclear but not mitochondrial genome involvement in 3-methylcholanthrene-induced expression of tumorigenicity in mouse somatic cells. Cancer Res. 49, 4715–4720.

Inoue, K., Nakada, K., Ogura, A., Isobe, K., Goto, Y., Nonaka, I., Hayashi, J.-I., 2000. Generation of mice with mitochondrial dysfunction by introducing mouse mtDNA carrying a deletion into zygotes. Nat. Genet. 26, 176–181.

Ishikawa, K., Takenaga, K., Akimoto, M., Koshikawa, N., Yamaguchi, A., Imanishi, H., Nakada, K., Honma, Y., Hayashi, J.-I., 2008. ROS-generating mitochondrial DNA mutations can regulate tumor cell metastasis. Science 320, 661–664.

Jacobs, H.T., 2003. The mitochondrial theory of aging: dead or alive? Aging Cell 2, 11–17.

Kaneda, H., Hayashi, J.-I., Takahama, S., Taya, C., Fischer Lindahl, K., Yonekawa, H., 1995. Elimination of paternal mitochondrial DNA in intraspecific crosses during early mouse embryogenesis. Proc. Natl. Acad. Sci. USA 92, 4542–4546.

Kasahara, A., Ishikawa, K., Yamaoka, M., Ito, M., Watanabe, N., Akimoto, M., Sato, A., Nakada, K., Endo, H., Suda, Y., Aizawa, S., Hayashi, J.-I., 2006. Generation of trans-mitochondrial mice carrying homoplasmic mtDNA with a missense mutation in a structural gene using ES cells. Hum. Mol. Genet. 15, 871–881.

Koshikawa, N., Iyozumi, A., Gassmann, M., Takenaga, K., 2003. Constitutive upregulation of hypoxia-inducible factor-1α mRNA occurring in highly metastatic lung carcinoma cells leads to vascular endothelial growth factor overexpression upon hypoxic exposure. Oncogene 22, 6717–6724.

Koshikawa, N., Maejima, C., Miyazaki, K., Nakagawara, A., Takenaga, K., 2006. Hypoxia selects for high-metastatic Lewis lung carcinoma cells overexpressing Mcl-1 and exhibiting reduced apoptotic potential in solid tumors. Oncogene 25, 917–928.

Kujoth, G.C., Hiona, A., Pugh, T.D., Someya, S., Panzer, K., Wohlgemuth, S.E., Hofer, T., Seo, A.Y., Sullivan, R., Jobling, W.A., Morrow, J.D., Van Remmen, H., Sedivy, J.M., Yamasoba, T., Tanokura, M., Weindruch, R., Leeuwenburgh, C., Prolla, T.A., 2005. Mitochondrial DNA mutations, oxidative stress, and apoptosis in mammalian aging. Science 309, 481–484.

Loeb, L.A., Wallace, D.C., Martin, G.M., 2005. The mitochondrial theory of aging and its relationship to reactive oxygen species damage and somatic mtDNA mutations. Proc. Natl. Acad. Sci. USA 102, 18769–18770.

Nakada, K., Inoue, K., Ono, T., Isobe, K., Ogura, A., Goto, Y.-i., Nonaka, I., Hayashi, J.-I., 2001. Inter-mitochondrial complementation: mitochondria-specific system preventing mice from expression of disease phenotypes by mutant mtDNA. Nat. Genet. 7, 934–940.

Niemann, S., Muller, U., 2000. Mutations in SDHC cause autosomal dominant paraganglioma, type3. Nat. Genet. 26, 268–270.

Pedersen, P.L., 1978. Tumor mitochondria and the bioenergetics of cancer cells. In: Wallach, D.F.H. (Ed.), Membrane Anomalies in Tumor Cells. Karger AG, Basel, pp. 190–274.

Penta, J.S., Johnson, F.M., Wachsman, J.T., Copeland, W.C., 2001. Mitochondrial DNA in human malignancy. Mutat. Res. 488, 119–133.

Polyak, K., Li, Y., Zhu, H., Lengauer, C., Willson, J.K.V., Markowitz, S.D., Trush, M.A., Kinzler, K.W., Vogelstein, B., 1998. Somatic mutations of the mitochondrial genome in human colorectal tumors. Nat. Genet. 20, 291–293.

Shay, J.W., Werbin, H., 1987. Are mitochondrial DNA mutations involved in the carcinogenic process? Mutat. Res. 186, 149–160.

Shitara, H., Hayashi, J.-I., Takahama, S., Kaneda, H., Yonekawa, H., 1998. Maternal inheritance of mouse mtDNA in interspecific hybrids: segregation of the leaked paternal mtDNA followed by the prevention of subsequent paternal leakage. Genetics 148, 851–857.

Takasu, M., Tada, Y., Wang, J.O., Tagawa, M., Takenaga, K., 1999. Resistance to apoptosis induced by microenvironmental stresses is correlated with metastatic potential in Lewis lung carcinoma. Clin. Exp. Metast. 17, 409–416.

Takenaga, K., Nakamura, Y., Sakiyama, S., 1997. Expression of antisense RNA to S100A4 gene encoding an S100-related calcium-binding protein suppresses metastatic potential of high-metastatic Lewis lung carcinoma cells. Oncogene 14, 331–337.

Taylor, R.W., Turnbull, D.M., 2005. Mitochondrial DNA mutations in human disease. Nat. Rev. Genet. 6, 389–402.
Trifunovic, A., Wredenberg, A., Falkenberg, M., Spelbrink, J.N., Rovio, A.T., Bruder, C.E., Bohlooly, Y.M., Gidlof, S., Oldfors, A., Wibom, R., Tornell, J., Jacobs, W.H., Larsson, N.G., 2004. Premature ageing in mice expressing defective mitochondrial DNA polymerase. Nature 27, 417–423.
Trifunovic, A., Hansson, A., Wredenberg, A., Rovio, A.T., Dufour, E., Khvorostov, I., Spelbrink, J.N., Wibom, R., Jacobs, H.T., Larsson, N.G., 2005. Somatic mtDNA mutations cause aging phenotypes without affecting reactive oxygen species production. Proc. Natl. Acad. Sci. USA 102, 17993–17998.
Wallace, D.C., 1999. Mitochondrial diseases in man and mouse. Science 283, 1482–1488.

FEBS Letters 582 (2008) 3525–3530

# Enhanced glycolysis induced by mtDNA mutations does not regulate metastasis

Kaori Ishikawa[a,b,1], Osamu Hashizume[a,1], Nobuko Koshikawa[c], Sayaka Fukuda[a], Kazuto Nakada[a], Keizo Takenaga[d], Jun-Ichi Hayashi[a,*]

[a] Graduate School of Life and Environmental Sciences, University of Tsukuba, 1-1-1 Tennodai, Tsukuba, Ibaraki 305-8572, Japan
[b] Japan Society for the Promotion of Science (JSPS), 8 Ichiban-cho, Chiyoda-ku, Tokyo 102-8472, Japan
[c] Division of Chemotherapy, Chiba Cancer Center Research Institute, 666-2 Nitona, Chuo-ku, Chiba 260-8717, Japan
[d] Shimane University Faculty of Medicine, 89-1 Enya-cho, Izumo, Shimane 693-8501, Japan

Received 4 August 2008; accepted 10 September 2008

Available online 19 September 2008

Edited by Veli-Pekka Lehto

**Abstract** **We addressed the issue of whether enhanced glycolysis caused by mtDNA mutations independently induces metastasis in tumor cells using mtDNA transfer technology. The resultant trans-mitochondrial cybrids sharing the same nuclear background of poorly metastatic carcinoma P29 cells, P29mtA11 and P29mtΔ cybrids, possessed mtDNA with a G13997A mutation from highly metastatic carcinoma A11 cells and mtDNA with a 4696 bp deletion mutation, respectively. The P29mtΔ cybrids expressed enhanced glycolysis, but did not express ROS overproduction and high metastatic potential, whereas P29mtA11 cybrids showed enhanced glycolysis, ROS overproduction, and high metastatic potential. Thus, enhanced glycolysis alone does not induce metastasis in the cybrids.**


*Keywords:* Pathogenic mtDNA mutation; mtDNA transfer technology; Trans-mitochondrial cybrid; Enhanced glycolysis; The Warburg effect; ROS overproduction; Metastasis

## 1. Introduction

Involvement of mtDNA mutations and the resultant mitochondrial respiration defects in tumor development have been suggested based on the evidence that most chemical carcinogens bind preferentially to mtDNA rather than to nuclear DNA [1–3]. Moreover, somatic mutations in mtDNA are accumulated preferentially in tumor cells rather than in normal cells of the same subjects [4,5], and many subsequent studies supported high frequencies of homoplasmic mutations in mtDNA of tumors [6–9].

On the contrary, our previous studies showed that mtDNA mutations were not involved in tumor development of cultured mouse [10,11] and human cells [12,13] using trans-mitochondrial cybrids obtained by mtDNA transfer between normal and tumor cells. The possibility that these observations represent some specific tumor cases can be excluded, since there has been no statistical evidence for the association of pathogenic mtDNA mutations and tumor development in the patients with mitochondrial diseases expressing respiration defects due to the pathogenic mtDNA mutations. The possibility of the involvement of polymorphic mtDNA mutations in tumor development also can be excluded, since there has been no statistical evidence for the presence of maternal inheritance of tumor development in spite of the strictly maternal inheritance of mammalian mtDNA [14,15].

However, it is still possible that mtDNA mutations are involved in other processes besides the oncogenic transformation of normal cells to develop tumors, such as the malignant progression of tumor cells to develop metastatic potential. Our recent study addressed this issue by means of mtDNA exchange technology, and demonstrated that mtDNA mutations inducing complex I defects and resultant overproduction of reactive oxygen species (ROS) reversibly controlled malignant progression of tumor cells to develop metastatic potential [16]. However, considering that complex I defects simultaneously induce enhanced glycolysis under normoxia (the Warburg effect) and ROS overproduction, it is necessary to determine whether the Warburg effect also controls metastasis independently. In fact, recent reports demonstrated that up-regulation of glycolysis caused by mutations or epigenetic controls of nuclear-coded genes regulate tumor phenotypes by the induction of a pseudo-hypoxic pathway under normoxia [17–20].

To address this issue, we generated trans-mitochondrial P29mtΔ cybrids by introduction of ΔmtDNA4696 with a 4696 bp deletion mutation into low metastatic Lewis lung carcinoma P29 cells. The P29mtΔ cybrids expressed mitochondrial respiration defects and enhanced glycolysis under normoxia, but did not express ROS overproduction, providing proper cellular system to examine whether the Warburg effect alone can control metastasis.

## 2. Materials and Methods

### 2.1. Cell lines and cell culture

The mouse cell lines and their characteristics are listed in Table 1. The P29 cells originated from Lewis lung carcinoma (C57BL/6 mouse strain), and B82 cells are fibrosarcoma cells derived from the L929 fibroblast cell line (C3H/An mouse strain). Parental cells, $\rho^0$ cells, and the trans-mitochondrial cybrids were grown in normal medium [DMEM + pyruvate (0.1 mg/ml) + uridine (50 mg/ml) + 10% fetal bovine serum].

*Corresponding author. Fax: +81 298 53 6614.
*E-mail address:* jih45@sakura.cc.tsukuba.ac.jp (J.-I. Hayashi).

[1]These authors contributed equally to this work.

0014-5793/$34.00 
doi:10.1016/j.febslet.2008.09.024

Table 1
Genetic characteristics of parent cells and their trans-mitochondrial cybrids

| Cell lines[a] | Nuclear genotypes (genetic marker)[b] | mtDNAgenotypes | Fusion combination | | | Selection |
|---|---|---|---|---|---|---|
| | | | Nuclear donors | × | mtDNA donors | |
| *Nuclear donors* | | | | | | |
| $\rho^0$P29 | P29 (HAT$^r$, BrdU$^s$) | mtDNA-less | | | | |
| *mtDNA donors* | | | | | | |
| B82mtP29 | B82 (HAT$^s$, BrdU$^r$) | Wild type | $\rho^0$B82 | × | en$^c$P29 | BrdU + UP$^-$ |
| B82mtA11 | B82 (HAT$^s$, BrdU$^r$) | G13997A | $\rho^0$B82 | × | enA11 | BrdU + UP$^-$ |
| B82mtΔ | B82 (HAT$^s$, BrdU$^r$) | ΔmtDNA4696 | $\rho^0$B82 | × | platelets | UP$^-$ |
| *Trans-mitochondrial cybrids* | | | | | | |
| P29mtP29 | P29 (HAT$^r$, BrdU$^s$) | Wild type | $\rho^0$P29 | × | enB82mtP29 | HAT + UP$^-$ |
| P29mtA11 | P29 (HAT$^r$, BrdU$^s$) | G13997A | $\rho^0$P29 | × | enB82mtA11 | HAT + UP$^-$ |
| P29mtΔ | P29 (HAT$^r$, BrdU$^s$) | ΔmtDNA4696 | $\rho^0$P29 | × | enB82mtΔ | HAT + UP$^-$ |

[a]As mtDNA donors, we used B82mtP29, B82mtA11, and B82mtΔ cybrids shearing the same nuclear background of B82 cells for excluding variations of nuclear-coded cytoplasmic factors in mtDNA donors. B82mtP29 cybrids carrying nuclear DNA from B82 cells and mtDNA from P29 cells were obtained by fusion of $\rho^0$B82 cells with enucleated P29 cells and subsequent cultivation in the selection medium with BrdU and UP$^-$. $\rho^0$B82 cells can survive in the selection medium with BrdU due to their lacking thimidine kinase activity, and cannot survive in the selection medium without uridine and pyruvate (UP$^-$ medium) due to their lacking mtDNA. Thus, BrdU and UP$^-$ eliminate unenucleated P29 cells and unfused $\rho^0$B82 cells, respectively, and allow exclusive growth of the B82mtP29 cybrids. B82mtΔ cybrids carrying nuclear DNA from B82 cells and ΔmtDNA4696 were obtained by fusion of $\rho^0$B82 cells with platelets from mito-mice carrying ΔmtDNA4696 [23] in the UP$^-$ selection medium. As G13997A mtDNA donors, we used B82mtA11 cybrids obtained in our previous work [16].
[b]All the mtDNA donors sharing the B82 nuclear background lacking thymidine kinase activity cannot survive in the presence of a hypoxanthine/aminopterin/thymidine (HAT). On the contrary, nuclear donors $\rho^0$P29 cells can grow in the HAT selection medium due to their processing thimidine kinase activity, but not in UP$^-$ selection medium due to their complete respiration defects by mtDNA depletion. Thus, HAT and UP$^-$ allow exclusive growth of the P29mtP29, P29mtA11, and P29mtΔ cybrids.
[c]en Represents enucleated.

### 2.2. Isolation of trans-mitochondrial cybrids

We isolated $\rho^0$ cells by treating parental cells with 1.5 mg/ml ditercalinium (DC), an antitumor bis-intercalating agent [21]. Complete depletion of mtDNA was confirmed by PCR analysis. Enucleated cells of the mtDNA donor were prepared by their pretreatment with cytochalasin B (10 μg/ml) for 10 min and centrifugation at 12000 × *g* for 30 min. Resultant cytoplasts were fused with $\rho^0$ cells by polyethylene glycol. Trans-mitochondrial cybrids were isolated in the selection medium that allows exclusive growth of the cybrids (see Table 1).

### 2.3. Genotyping of mtDNAs

Transfer of mtDNAs in the cybrids was confirmed by RFLP analysis of the PCR products and Southern blot analysis. For recognition of the G13997A mutation, a 147-bp fragment containing the 13997 site was amplified by PCR. The nucleotide sequences from n.p. 13963 to 13996 (CCCACTAACAATTAAACCTAAACCTCCATActTA, small letters indicate the mismatch site) and n.p. 14109 to 14076 (TTCATGTCATTGGTCGCAGTTGAATGCTGTGTAG) were used as oligonucleotide primers. Combination of the PCR-generated mutation with the G13997A mutation creates a restriction site for *Afl* II, and generates 114-bp and 33-bp fragments on *Afl* II digestion. The restriction fragments were separated in 3% agarose gel. To estimate the proportion of ΔmtDNA, we carried out Southern blot analysis. Total DNAs (3 μg) extracted from cybrids were digested with the restriction enzyme *Xho* I. Restriction fragments were separated in 0.8% agarose gel, transferred to a nylon membrane, and hybridized with alkaline phosphatase-labeled mouse mtDNA probes (n.p. 1751–3803). Probe labeling and signal detection were carried out as described in the protocols of the Alk-Phos Direct (GE Healthcare, Buckinghamshire, UK). For quantification of ΔmtDNA, we use the NIH IMAGE program.

### 2.4. Biochemical measurement of respiratory enzyme activities

Cells in log-phase growth were harvested, and the respiratory complexes were assayed as described before [22]. Briefly, NADH and cytochrome *c* (oxidized form) were used as substrates for estimation of complexes I + III activity, and the reduction of cytochrome *c* was monitored at 550 nm. For estimation of complexes II + III activity, sodium succinate and cytochrome *c* (oxidized form) were used as substrates, and reduction of cytochrome *c* was monitored at 550 nm. For estimation of complex IV activity, cytochrome *c* (reduced form) was used as substrates, and the enzyme activity was determined by monitoring the oxidation of cytochrome *c* at 550 nm.

### 2.5. Measurement of ROS production

ROS generation was detected with mitochondrial superoxide indicator MitoSOX-RED (Invitrogen, Carlsbad, CA, USA). Cells were incubated with 5 μM MitoSOX-RED for 10 min at 37 °C in serum-free DMEM, washed twice with Dulbecco's phosphate-buffered saline (DPBS), and then immediately analyzed with a FACS can flow cytometer (Becton Dickinson, Mountain View, CA, USA).

### 2.6. SDS–PAGE and Western blotting

To detect MCL-1, cells were lysed on ice for 10 min in 1% Triton X-100, 1% sodium deoxycholate, 0.1% SDS, 50 mM Tris–HCl (pH 7.5), 150 mM NaCl, 1 mM PMSF, and protease inhibitor cocktail (Sigma–Aldrich, St. Louis, MO, USA). After centrifugation at 10000 × *g* for 10 min at 4 °C, the supernatant was used as a sample. Proteins were resolved by SDS–PAGE under reducing conditions. The resolved proteins were transferred electrophoretically to a nitrocellulose membrane. After incubation with 5% dry milk in TBS-T [150 mM NaCl, 50 mM Tris–HCl (pH 7.4), 0.05% Tween 20] for at least 1 h at room temperature, the membrane was incubated with polyclonal anti-MCL-1 antibody (Santa Cruz Biotechnologies, Inc., Santa Cruz, CA, USA) for 1 h at room temperature, washed extensively with TBS-T, and then incubated with horseradish peroxidase-conjugated goat anti-rabbit IgG. Proteins were detected using ECL Western blotting detection reagents (GE Healthcare). For loading controls, the membrane was stripped, and subsequently incubated with monoclonal anti-β-actin antibody (Sigma–Aldrich) followed by incubation with horseradish peroxidase-conjugated goat anti-mouse IgG.

### 2.7. Measurement of the concentration of lactate in the cell medium

Cells were seeded at $5 \times 10^4$ cells/well of a 6-well plate and cultured for 24 h. The amounts of lactate in the cell medium were estimated using an F-kit L-Lactic acid (Roche, Basel, Switzerland).

### 2.8. Assays of metastatic potential

To test experimental metastatic potential, $5 \times 10^5$ cells/100 μl PBS were injected into the tail vein of 6-week-old male C57BL/6 mice (CLEA Japan, Tokyo, Japan). The mice were sacrificed 18 days later, and their lungs were removed. The lungs were fixed in the Bouin's solution, and parietal nodules were counted.

## 3. Results

### 3.1. Isolation of the mtDNA donors sharing the same nuclear background of B82 cells

This study examined whether the Warburg effect induced by mitochondrial respiration defects alone controls metastasis in mouse Lewis lung carcinoma cells. For this, we used mtDNA-less ($\rho^0$) P29 cells derived from poorly metastatic Lewis lung carcinoma P29 cells as nuclear DNA donors and mtDNA recipients (Table 1).

As mtDNA donors, we isolated trans-mitochondrial B82mtP29, B82mtA11, and B82mtΔ cybrids shearing the same nuclear background of B82 cells (Table 1). The B82mtP29 cybrids carrying nuclear DNA from B82 cells and mtDNA from P29 cells were obtained by fusion of $\rho^0$B82 cells with enucleated P29 cells (Table 1). The B82mtΔ cybrids carrying nuclear DNA of B82 cells and ΔmtDNA4696 were obtained by fusion of $\rho^0$B82 cells with platelets from mito-mice carrying ΔmtDNA4696 [23]. The B82mtA11 cybrids isolated in our previous work [16] were obtained by fusion of $\rho^0$B82 cells with enucleated A11 cells.

These cybrids are appropriate to be used as mtDNA donors to $\rho^0$P29 cells by the following two reasons. One is that the cybrids sharing the B82 nuclear background can exclude the influence of variations of the nuclear-coded cytoplasmic factors on metastasis of the mtDNA recipient $\rho^0$P29 cells. Another is that the cybrids sharing B82 nuclear background lack thymidine kinase activity, and cannot survive in the presence of a hypoxanthine/aminopterin/thymidine (HAT). Thus, unenucleated mtDNA donor cybrids can be excluded in the selective medium with HAT (Table 1).

### 3.2. Isolation of trans-mitochondrial cybrids carrying mtDNA with pathogenic mutation

These mtDNA donor cybrids were used for obtaining the trans-mitochondrial cybrids, P29mtP29, P29mtA11, and P29mtΔ (Table 1). First, we isolated trans-mitochondrial P29mtΔ cybrids, possessing the nuclear genome of the P29 cells and mitochondrial genome of ΔmtDNA4696 with a 4696 bp deletion mutation, by the fusion of the $\rho^0$P29 cells with enucleated B82mtΔ cybrids (Table 1). Our previous reports showed that accumulation of the ΔmtDNA4696 induced suppression of overall mitochondrial translation due to the large-scale deletion mutation including five mitochondrial tRNA genes from ΔmtDNA4696 [23,24]. Therefore, we expected that the P29mtΔ cybrids with ΔmtDNA4696 would express enhanced glycolysis under normoxia, but not express ROS overproduction, probably due to overall mitochondrial respiration defects induced by ΔmtDNA4696. Thus, the P29mtΔ cybrids would provide an ideal system to examine whether enhanced glycolysis alone could induce metastasis in poorly metastatic P29 cells.

We also obtained trans-mitochondrial P29mtA11 and P29mt29 cybrids by the fusion of the $\rho^0$P29 cells with enucleated B82mtA11 and B82mtP29 cybrids for using as positive and negative controls of metastasis, respectively (Table 1). Our recent report [16] isolated P29mtA11 and P29mtP29 cybrids by the fusion of $\rho^0$P29 with enucleated A11 cells and P29 cells, respectively, and showed that the P29mtA11 cybrids were highly metastatic and P29mt29 cybrids were poorly metastatic. However, it was possible that some cytoplasmic factors encoded by nuclear DNA may affect metastatic potentials,

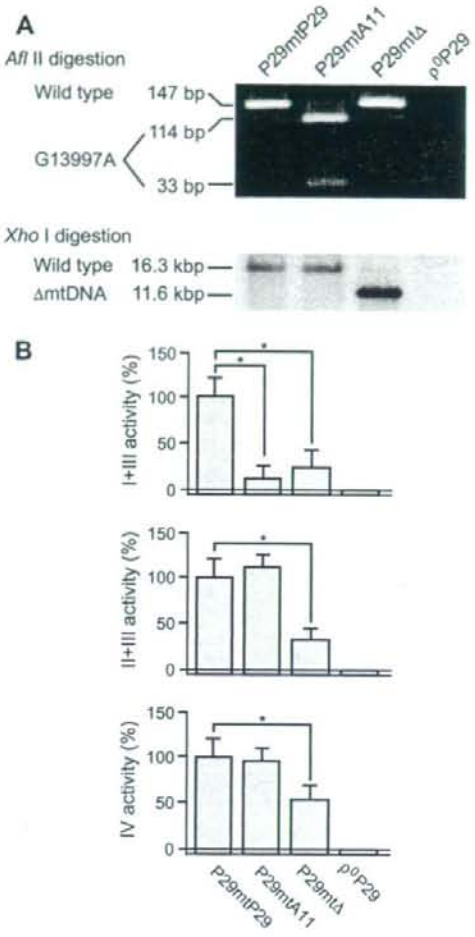


Fig. 1. Genotyping of mtDNA and respiratory complex activities. (A) Identification of the mtDNA genotypes. Upper panel: For identification of A11 mtDNA with the G13997A mutation, the PCR products were digested with *AflII*. The PCR products of the mtDNA with the G13997A mutation from A11 cells produce 114- and 33-bp fragments because of the gain of an *AflII* site by a G13997A substitution, whereas those of mtDNA without the mutation produce a 147-bp fragment due to the absence of the *AflII* site. Lower panel: For estimation of ΔmtDNA4696 proportions in the cybrids, we used Southern blot analysis of total DNA digested with the restriction endonuclease *Xho* I. Fragments of 16.3 kbp and 11.6 kbp correspond to wild-type mtDNA and ΔmtDNA4696, respectively. (B) Biochemical analysis of respiratory complex activities. Respiratory complex I (NADH dehydrogenase), complex II (succinate dehydrogenase), complex III (cytochrome *c* reductase), and complex IV (cytochrome *c* oxidase) are components of electron-transport chain, and are located in the mitochondrial inner membrane. Mitochondrial respiratory function was examined by estimating their activities. Since the activity of complexes II + III is normal in the P29mtA11 cybrids, reduced activity of complexes I + III in them should result from complex I defects. Bars represent the means ± S.D. ($n = 3$). *, $P < 0.05$.

since nuclear background of mtDNA donor A11 and P29 cells are different from each other. This study can exclude this possibility by the use of the B82mtA11 and B82mtP29 cybrids

sharing the same nuclear background of B82 cells as mtDNA donors.

### 3.3. mtDNA genotypes and resultant phenotypes of respiratory function in the cybrids

Using PCR and Southern blot analyses, we carried out the mtDNA genotyping of the P29mtP29, P29mtA11, and P29mtΔ cybrids (Fig. 1A). The G13997A mutation in mtDNA from A11 cells creates an *Afl* II site in PCR products amplified using mismatch primers [16]. Therefore, we carried out *Afl* II digestion of their PCR products, and showed that mtDNA in P29mtA11 cybrids possessed a homoplasmic G13997A mutation, while mtDNA in P29mtP29 and P29mtΔ cybrids did not (Fig. 1A, upper panel). The ΔmtDNA4696 was identified by Southern blot analysis. The results showed that P29mtΔ cybrids possessed 88% ΔmtDNA4696, while the P29mtP29 and P29mtA11 cybrids did not have any ΔmtDNA4696 (Fig. 1A, lower panel). As expected, no mtDNA was found in parental $\rho^0$P29 cells (Fig. 1A).

Then, their mitochondrial respiratory function was examined by estimating activities of mitochondrial respiratory complexes (Fig. 1B). Parental $\rho^0$P29 cells and P29mtΔ cybrids showed overall respiration defects due to complete mtDNA depletion and accumulation of ΔmtDNA4696 possessing a 4696 bp-deletion mutation, respectively. Specific reduction of complex I activity was exclusively observed in P29mtA11 cybrids, while P29mtP29 cybrids showed normal mitochondrial respiratory function (Fig. 1B).

### 3.4. Effects of respiration defects on ROS production and nuclear-coded MCL-1 expression

Since we have reported recently [16] that ROS overproduction and resultant up-regulation of nuclear-coded antiapoptotic MCL-1 (myeloid cell leukemia-1), at least in part, are responsible for metastasis, we estimated the amounts of ROS and the nuclear-coded MCL-1 in the cybrids (Fig. 2). The P29mtΔ cybrids did not show ROS overproduction (Fig. 2A) and up-regulation of MCL-1 (Fig. 2B). Similar results were obtained in $\rho^0$P29 cells and the P29mtP29 cybrids (Fig. 2B). On the contrary, the P29mtA11 cybrids expressing complex I defects showed ROS overproduction (Fig. 2A) and upregulation of MCL-1 (Fig. 2B). These observations suggest that ROS overproduction and up-regulation of MCL-1 cannot be induced by overall mitochondrial respiration defects or normal respiratory function.

### 3.5. Effects of mitochondrial respiration defects on glycolytic activity and metastasis

Then, we examined the glycolytic activity of these cybrids and parental $\rho^0$P29 cells by estimating lactate level in their culture medium. As expected, parental $\rho^0$P29 cells and P29mtΔ cybrids expressing overall respiration defects (Fig. 1B) showed significant overproduction of lactate (Fig. 3A). Slight overproduction of lactate was observed in P29mtA11 cybrids expressing complex I defects, while P29mtP29 cybrids showed normal lactate secretion (Fig. 3A). These observations suggest that $\rho^0$P29 cells and P29mtΔ cybrids expressed enhanced glycolysis under normoxia, i.e., the Warburg effect, due to overall mitochondrial respiration defects, but did not express ROS overproduction. Thus, they can be used for determination of whether the Warburg effect alone induces high metastatic potential in tumor cells.

Finally, we examined metastatic potentials by inoculation of the cybrids into the tail vein of male C57BL/6 mice and counting the number of nodules formed in the lung 18 days after inoculation. The $\rho^0$P29 cells and P29mtΔ cybrids expressing the Warburg effect, but not expressing ROS overproduction did not form lung nodules (Fig. 3B). As expected from our recent report [16], P29mtA11 cybrids expressing the Warburg effect and ROS overproduction formed nodules in the lung,

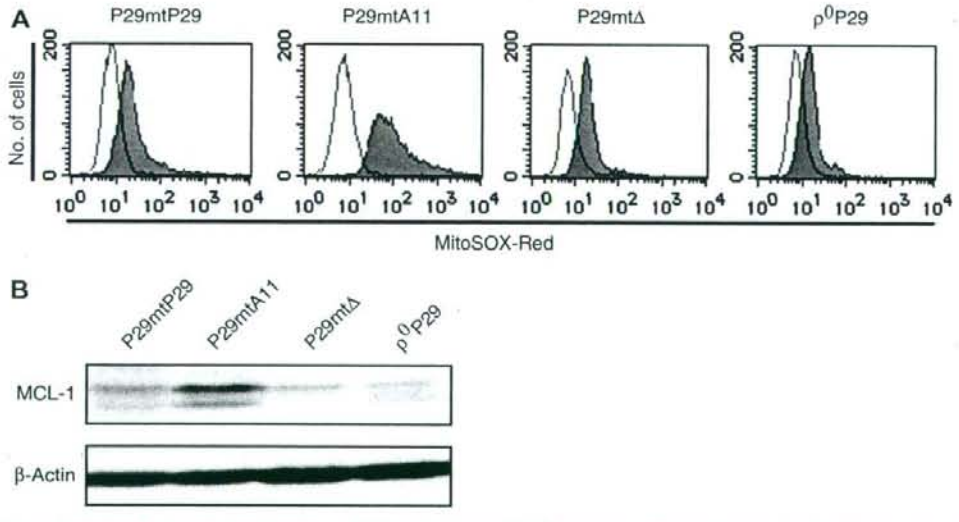


Fig. 2. Effects of mitochondrial respiratory function on ROS production and MCL-1 expression. (A) Estimation of ROS production. We carried out flow-cytometric analysis using $1 \times 10^6$ cells. Cells treated with 5 μM MitoSOX-RED were subjected to FACScan for quantitative estimation of superoxide. (B) Expression of nuclear-coded MCL-1 by Western blot analysis. We used β-actin as loading control in the Western blots.